Three-dimensional Hydrodynamic Modelling of the Impact of Macrophytes in Lake Saint-Pierre

Maxim Bulat

A Thesis

in the Department

of

Geography, Planning and Environment

Presented in Partial Fulfillment of the Requirements

For the Degree of Masters of Science

(Geography, Urban and Environmental Studies) at

Concordia University

Montreal, Quebec, Canada

October 2018

CONCORDIA UNIVERSITY

School of Graduate Studies

This is to certify that the thesis prepared

By: Maxim Bulat

Entitled: Three-dimensional hydrodynamic modelling of the impact of macrophytes in Lake Saint-Pierre

and submitted in partial fulfillment of the requirements for the degree of

Master of Science (Geography, Urban and Environmental Studies)

complies with the regulations of the University and meets the accepted standards with respect to originality and quality.

Signed by the final Examining Committee:

_____ Dr. Norma Rantisi	Chair
_____ Dr. S. Samuel Li	External Examiner
_____ Dr. Jeannine-Marie St-Jacques	Examiner
_____ Dr. Pascale Biron	Supervisor
_____ Dr. Jay Lacey	Supervisor

Approved by _____
Chair of Department or Graduate Program Director

_____ 2018 _____
Date Dean of Faculty

ABSTRACT

Three dimensional hydrodynamic modelling of the impact

of macrophytes in Lake Saint-Pierre

Maxim Bulat

Aquatic plants (macrophytes) are known to affect flow dynamics by contributing to flow resistance. Most studies on flow-vegetation interactions are performed in laboratory flumes and focus on the flow field around simulated plants. Little research is done at the level of real vegetation patches in water bodies such as Lake Saint-Pierre (LSP), a large fluvial lake of the Saint-Lawrence River in Quebec, Canada. Although some two-dimensional (2D) hydrodynamic models have included additional drag due to macrophytes in natural rivers through an increase in roughness coefficient (Manning's *n*), these studies do not well represent the near-zero velocities observed in dense macrophyte zones such as those of LSP. Furthermore, because most submerged plants are flexible and have different growth forms and heights, a three-dimensional (3D) approach may better represent their true impact on the flow field. The objective of this study is to develop a 3D hydrodynamic model (Delft3D) of a large-scale field site with abundant macrophytes (LSP) and investigate to what extent the flow and residence time are affected by macrophytes. Two macrophyte simulation approaches (trachytope and modified k-ε turbulence closure model) were first compared to laboratory experiments from the literature to determine how best to simulate the macrophyte impact on flow dynamics. Results indicated that the modified k-ε turbulence approach better predicted the variability of the flow field. This approach was then used to study the zone at the mouth of the Saint François

River in LSP, where an extensive macrophyte zone is present annually. Results showed a marked increase in residence time in the zone affected by macrophytes when using the modified *k-ε* turbulence closure model compared to the Manning's *n* approach, particularly near the bed. An improved agreement with field measured depth-averaged velocity is obtained with this novel approach (correlation coefficient of 0.80 compared to 0.46 with Manning's *n* only). In addition, a good fit was obtained between vertical velocity profiles modelled and measured in the macrophyte zone. Sensitivity analysis revealed that the additional drag due to plants was closely associated with plant height, but that plant density played only a minor role in current reduction. These findings indicate that it is possible to accurately quantify both the horizontal and vertical differences in flow resulting from submerged vegetation in large fluvial systems.

Acknowledgements

I would like to express my sincere gratitude to my supervisors Dr. Pascale Biron and Dr. Jay Lacey, whose continuous support, patience and guidance has made the learning process of this thesis a positive experience and personal life achievement. I would also like to thank Guénolé Choné for providing his technical assistance in all software related challenges I faced at the beginning of my program. Also, for their expertise in biology I would like to thank Morgan Botrel, Dr. Christiane Hudon and Dr. Roxane Maranger. Their insightful commentaries provided invaluable contribution in the manuscript preparation. I am appreciative of Morgan Botrel who provided unpublished field data regarding velocity and submerged aquatic vegetation biomass and height measurements used in this project. Thanks to NSERC Discovery Grants to Dr. Pascale Biron, Dr. Jay Lacey, and, Dr. Roxane Maranger, FRQNT, Concordia University and GRIL for the financial support which allowed me to focus more on this work. I am forever grateful to my wife Rodica and my family who supported and never gave up on me during these years.

Contribution of Authors

Chapter 6:

Co-Authors:

Pascale M. Biron, Jay R. Lacey, Morgan Botrel, Christiane Hudon and Roxane Maranger

Table of Contents

List of Figures

List of Tables

1. Introduction

Lake Saint-Pierre (LSP), a freshwater widening of the St. Lawrence River (SLR) located downstream of the greater Montreal area, is a critical area for wildlife and aquatic species (Hudon and Carignan, 2008). The lake was chosen as Ramsar site in 1998 (the Ramsar Convention on global conservation of wetlands, Ramsar Sites Information Service, 2017), and in 2000 it was designated as UNESCO Biosphere Reserve (Canadian Commission for UNESCO, 2017).

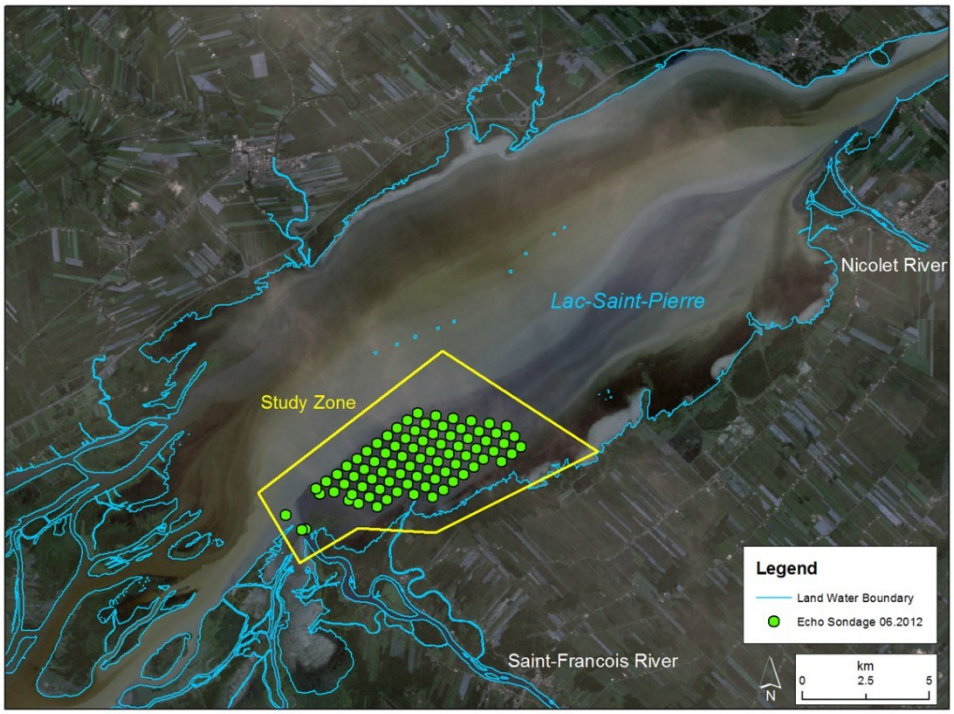

Figure 1.1. Lake Saint-Pierre and the study zone (in red) indicating where field measurements (velocity, depth, turbidity, macrophyte biomass) have been taken during GRIL field campaigns.

It accumulates the flow from numerous tributaries such as the l'Assomption, Chicot, Maskinongé, du Loup, and Yamachiche Rivers (north shore) and the Richelieu, Yamaska, Saint-François and Nicolet Rivers (south shore). Upstream of LSP, the SLR is heavily affected by five

dams built in the last century (Moses-Saunders Power Dam, Carillon Generating Station, Beauharnais, Des Cèdres and Rivière-des-Prairies). The upstream section of the lake is characterized by a complex of islands and channels known as the Berthier-Sorel archipelago (Figure 1.1). Most of the lake is relatively shallow, with an average depth of 3-4 m. A significant portion of the flow goes through a man-made central channel with depths exceeding 11 m, which allows navigation through the area (Hudon and Carignan, 2008). The surface of LSP covers around 300 km^2 and stretches for nearly 30 km in length. Approximately 260 km^2 of the lake is covered by submerged aquatic plants (macrophytes) during July-August, covering 85% of the total area of the LSP (Hudon and Carignan, 2008). The predominant species found in the lake are *Vallisneria americana* (wild celery), *Potamogeton richardsonii* (Richardson's pondweed), *Stuckenia pectinate* (sago or fennel pondweed, or ribbon weed), *Elodea nuttallii* (western waterweed or Nuttall's waterweed), and *Heteranthera dubia* (water stargrass or grassleaf mudplantain) (Figure 1.2).

Figure 1.2. The predominant macrophyte species found in Lake Saint-Pierre: A - *Vallisneria americana* (Fredlyfish4, 2016), B - *Potamogeton richardsonii* (eMonocot Team Classification, 2018), C - *Stuckenia pectinate* (Lamiot, 2017), D - *Elodea nuttallii* (Fischer, 2011), and E - *Heteranthera dubia* (Fritzflohrreynolds, 2012)

Since the 1950s, Lake Saint-Pierre and the St. Lawrence River have experienced pressure caused by intensive urbanization and agriculture as well as physical modifications. In addition, LSP is affected by urban waste pollution from the municipal effluent coming from the Montreal Wastewater Treatment Plant, which discharges daily approximately 3.54 million m^3 (41 m^3/s) of treated wastewater containing suspended particulate matter and phosphorus (Blaise et al., 2008; Marcogliese et al., 2015).

The water quality in LSP is affected by the agricultural runoff transported by the tributaries that pass through the farmlands surrounding the lake (Roy, 2002; Hudon and Carignan, 2008; Boyer et al., 2010). At the mouth of the Yamaska and Saint-François Rivers, filamentous green algae (FGA) blooms are often observed due to the excessive concentrations

of nutrients and low flow stage (Cattaneo et al., 2013). Furthermore, farm field erosion results in large volumes of fine suspended sediments transported by the tributaries. The overall habitat deterioration led to the well-documented population crash of Yellow perch (Perca flavescens) (Boyer et al., 2010; Giraudo et al., 2016).

Many studies show that velocity is affected and reduced in zones with abundant submerged vegetation (Boudreau et al., 1994; Morin et al., 2000b; Morin et al., 2003; Marjoribanks et al., 2014b; Marjoribanks et al., 2017). The abundance of submerged aquatic plants increases local flow resistance resulting in higher water levels (Boothroyd et al., 2015). Velocity as a hydraulic parameter is a critical component in local river discharge estimation. An accurate estimate of velocity and discharge is in turn needed to better understand the role of macrophytes on the spatial variation and dynamics of nutrient and pollutant concentrations: leading to better estimates of nutrient fluxes and budgets in rivers and lakes (Janse, 1997; Billen et al., 2001; Justić et al., 2002; Garnier et al., 2005; Hudon and Carignan, 2008).

2. Literature review

2.1 Macrophyte representation

Most of the studies on the impact of vegetation on the flow dynamics have used a simplified representation of plants in a laboratory setting (Wilson and Horritt, 2002; Järvelä, 2003; James et al., 2004; Righetti, 2008; Dijkstra and Uittenbogaard, 2010; King et al., 2012). Within laboratory experiments, only a few studies used real vegetation and even fewer studies have been conducted which consider vegetation in the field and only in emergent conditions (Ree and Crow, 1977; Nikora et al., 2008; Vargas-Luna et al., 2015). Vargas-Luna et al. (2015) reviewed 743 laboratory tests with artificial plants and 279 with real vegetation including some field surveys. The authors tested existing models of emerged and submerged macrophytes and compared the predictions with an extensive dataset. They concluded that the degree of submergence of aquatic vegetation is the principal parameter for the global flow resistance. Out of the tested models, the model by Baptist (2005) demonstrated equally good performance for both submerged and emergent conditions.

The laboratory studies can be further divided into three conventionally applied patterns, staggered, parallel and random, each approximating the spatial distribution of plants (Figure 2.1). Examples of studies where artificial plants were arranged linearly are Kubrak et al. (2008), Nezu and Sanjou, (2008), Velasco et al. (2008), Yan (2008), Dijkstra and Uittenbogaard (2010) and Okamoto and Nezu (2010). Random patterns were investigated by Murphy et al. (2007) and King et al. (2012), whereas Liu et al. (2008), Yang (2008) and Cheng (2011) examined a staggered pattern. Regardless of the patterns chosen, these laboratory experiments remain simplistic and, as Vargas-Luna et al. (2015) pointed out, unrealistic.

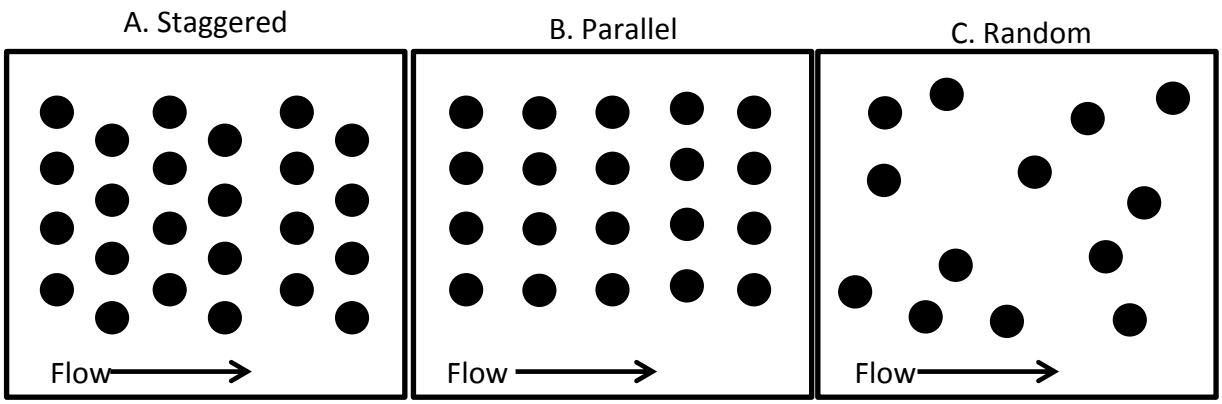

Figure 2.1. Spatial patterns used in laboratory experiments, black circles represent rigid cylinders. Reproduced from Vargas-Luna et al. (2015)

The use of rigid cylinders to simulate plants is very common, with only few studies representing plants as flexible strips (Dijkstra and Uittenbogaard, 2010) and as a complex voxelized (as pixels in a three-dimensional environment) 3D point cloud (Boothroyd et al., 2017). Rigid-cylinder models, which predict flow-resistance, deal with vegetation that is submerged (Klopstra et al., 1997; Huthoff, 2007; Yang and Choi, 2010), emergent (Petryk and Bosmajian, 1975, Ishikawa et al., 2003, Hoffmann, 2004; James et al., 2004) or both simultaneously (Stone and Shen, 2002; Baptist, 2005; Cheng, 2011).

It has long been known that vegetation affects the total shear stress in rivers. Schlichting (1936) suggested splitting the total shear stress into stress due to vegetation and bed-shear stress to assess flow resistance in open vegetated channels, a method which became widely accepted by other researchers. Similarly, Raupach (1992) suggested expressing bed shear stress as a fraction of the total shear stress to analytically predict flow resistance.

Quantifying the hydrodynamic impacts of macrophytes for large waterbodies remains a challenge. Resistance predictors commonly include the drag caused by vegetation, which

contains the apparent drag coefficient, C_D, a dimensionless constant of proportionality estimated for a given set of hydraulic conditions (Hygelund and Manga, 2003; Vargas-Luna et al. 2015). Since most macrophytes are supple and undergo reconfiguration (reacting to an increase in flow pressure by bending stems or long leaves), their presence affects C_D and in turn the estimation of the flow resistance once a plant flexes. In turn, the apparent drag coefficient and flow resistance were shown to vary markedly with differences in stem width and length, as well as structural plant rigidity or flexibility, plant posture (Boothroyd et al., 2017), and the amount of foliage (Vargas-Luna et al., 2015). Differences in experimental techniques, study design and measurement methods/equipment account for the large range of apparent drag coefficients obtained from previous studies. The apparent drag coefficient for plants has been estimated as a function of velocity (Sand-Jensen, 2003; O'Hare et al., 2007; Wunder et al., 2011) and as a function of the Reynolds number, Re. Values of Re are estimated either using inundated depth of vegetation and average velocity (Wu et al., 1999; Wilson, 2007; 2017), or through other dimensions pertinent to aquatic vegetation, such as stem thickness or diameter. For example, stem thickness and diameter have been used in combination with either average flow through vegetation (Tanino and Nepf, 2008; Kothyari et al., 2009; Cheng and Nguyen, 2011) or average velocity (Wilson and Horritt, 2002; Armanini et al., 2005).

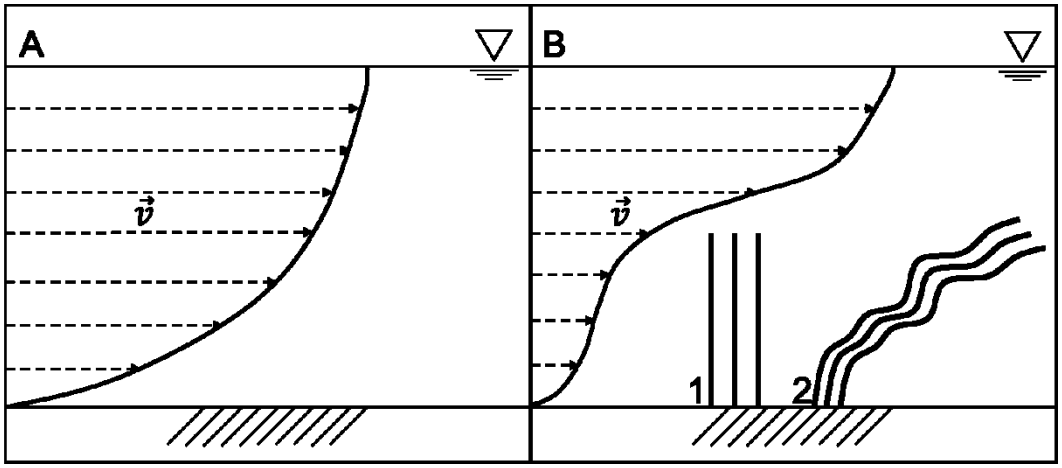

Figure 2.2. The schematic representation of the vertical velocity profile (A) and the drag due to the submerged vegetation characterized as rigid cylinders (B.1) and flexible stripes (B.2). Reproduced from Vargas-Luna et al. (2015).

In many studies, special attention has been paid to characterize the vertical velocity profile and its shape (Aberle and Järvelä, 2013; Hu et al., 2013) as it is affected by the vegetation. For emergent vegetation, the profile shape is mostly attributed to the density and the vertical distribution of foliage (Vargas-Luna et al., 2015); whereas in the case of submerged macrophytes (Figure 2.2B), it depends on the density and flexibility of plants as well as the submergence degree represented by a ratio of plant height to total water depth (Nepf, 2012a,b). Since the vertical velocity profile represents several vertical zones due to the presence of macrophytes (Figure 2.2B), several layers may need to be defined and treated separately in modelling due to different velocity and macrophyte properties (Vargas-Luna et al., 2015).

2.2 Study scale

Nepf (2012b) distinguishes at least three scales for the study of macrophytes – individual plant blades and stems, plant canopies of finite area, and reach scale, where, as the researcher argues, "the flow resistance is more connected to the patchiness of the submerged vegetation than the geometry of individual plants" (p. 262). There is insufficient attention paid to the effects of submerged vegetation on flow at the scale of real vegetation patches (Marjoribanks et al., 2017). Existent models are built on physically-based empirical relationships using roughness parameters such as Manning's *n* and do not reflect spatial variation within the flow field (Marjoribanks et al., 2017).

A theory on how to represent the impact of macrophytes on flow on a reach scale has been introduced by Pitlo and Dawson (1990) who argue that vegetation stands introduce a blockage factor and increase in-channel resistance by obstructing flow. The suggested blockage factor (proportion of a river reach occupied by submerged vegetation) could be determined through a single cross section, surface area, or volumetrically (Green, 2005a). The first two offer two-dimensional measures and thus are limited to two-dimensional modelling. While the volumetric approach offers a three-dimensional perspective on macrophyte-flow interactions, it is biased by variation of channel bed within a plant stand (Green, 2005b). Considering these limitations, Green (2005b) suggests representing the blockage factor through multiple cross-sections to account for bathymetry variability. The weighted median of all cross-sectional blockage factors produced the strongest non-linear relationship with vegetation resistance in a certain site, although more tests are needed since a single species *Ranunculus* (water-crowfoot) was used (Green, 2005b). While this method appears to work in certain reaches, it is

challenging to obtain the bathymetry/cross-sections in larger non-wadable streams in the presence of macrophytes.

Computational Fluid Dynamics (CFD) offers the potential to improve our understanding of flow-macrophyte relations in vegetated watercourses (Marjoribanks et al., 2014a). For example, Marjoribanks et al. (2017) and Boothroyd et al. (2017) developed a technique termed the Mass Flux Scaling Algorithm (MFSA) to represent submerged vegetation in a model based on the Reynolds averaged Navier-Stokes (RANS) equations. Marjoribanks et al. (2017) reported mixed results, with some of the locations showing good agreement between model predictions and field data whereas other locations had poorer agreement due to errors in geolocation, field measurement, or model discretization. This approach, however, is focused on flow–plant interactions at the level of individual plants, and is not applicable at the scale of LSP.

The integration of submerged vegetation in numerical models requires a numerical grid of high enough resolution to represent individual plants in an open vegetated channel, which introduces other problems. Higher-resolution numerical grids increase calculation time substantially and require powerful computers or even computer clusters to deal with multiple equations per time step. Brito et al. (2016) and Boothroyd et al. (2017) argue that submerged vegetation could be represented as porous media due to how dense it is, thus eliminating the need of a high-resolution grid. The experiment carried out by Brito et al. (2016) represents submerged vegetation as a porous layer whereas Boothroyd et al. (2017) focus on a dynamic volumetric representation of a single plant. Brito et al. (2016) used a 10-m long compound laboratory open channel with a numerical grid consisting of 1000 longitudinal, 80 vertical and 200 lateral elements (160,000,000 in total). This is therefore still a high-resolution grid category.

The porous media flow is represented by the volumetric mean of RANS equations, which are used for free flow description. Although Brito et al. (2016) focused their study on the inundated floodplain, they argue it could be applied to any open channel which has submerged vegetation. They found good agreement between the experimental and numerical bed-averaged velocity in both plant-height scenarios although discrepancies in velocity are observed locally in the flow. Overall, however, the effect of submerged vegetation on the flow field was accurately estimated. This is therefore an alternative approach to macrophyte integration into 3D models as it allows addressing the spatial heterogeneity and presence of uncertainty linked to the drag coefficient. Since the experiment has been performed in a rectangular laboratory channel, this approach necessitates further validation for different channel shapes, macrophyte flexibility and level of vegetation density. It remains unclear if this approach is applicable at the scale of a significantly larger waterbody such as LSP.

2.3 Existing model of Lake St. Pierre

Currently the Hydrology and Ecohydraulic Section of Environment and Climate Change Canada (ECCC) uses a two-dimensional (2D) hydrodynamic model for the SLR, which includes LSP (Martin et al., 2016). It was built with the help of an eco-hydraulics software suite called H2D2 (Hydrosim2-Dispersim2), which is a modular software developed by Yves Secretan and Jean Morin and supported by the INRS-ETE (Institut National de Recherche Scientifique, Centre Eau-Terre-Environnement). H2D2 uses Saint-Venant equations derived for shallow water simulations (Morin et al., 2000a; b; 2003; Secretan and Dubos, 2005) where the scale of horizontal length is considered to be significantly larger than the vertical length scale and thus

the depth component is omitted, assuming constant velocity throughout the water column (i.e., 2D). H2D2 characterizes the drag due to the submerged vegetation through the Manning's *n* friction coefficient (Boudreau et al., 1994; Talbot, 2006). Although raising the value of this coefficient reduces velocity, it cannot result in near-zero velocities, as are observed in some parts of LSP.

Since the model H2D2 is used to simulate flow in the SLR between Cornwall and Quebec City, it has a relatively coarser grid in the area at the mouth of the SFR (Figure 2.3). It is therefore not clear if this model can accurately simulate the complex flow field in the zone affected by macrophytes. Furthermore, being a depth-averaged model, it obviously cannot represent the vertical variability of velocity in the macrophyte zone.

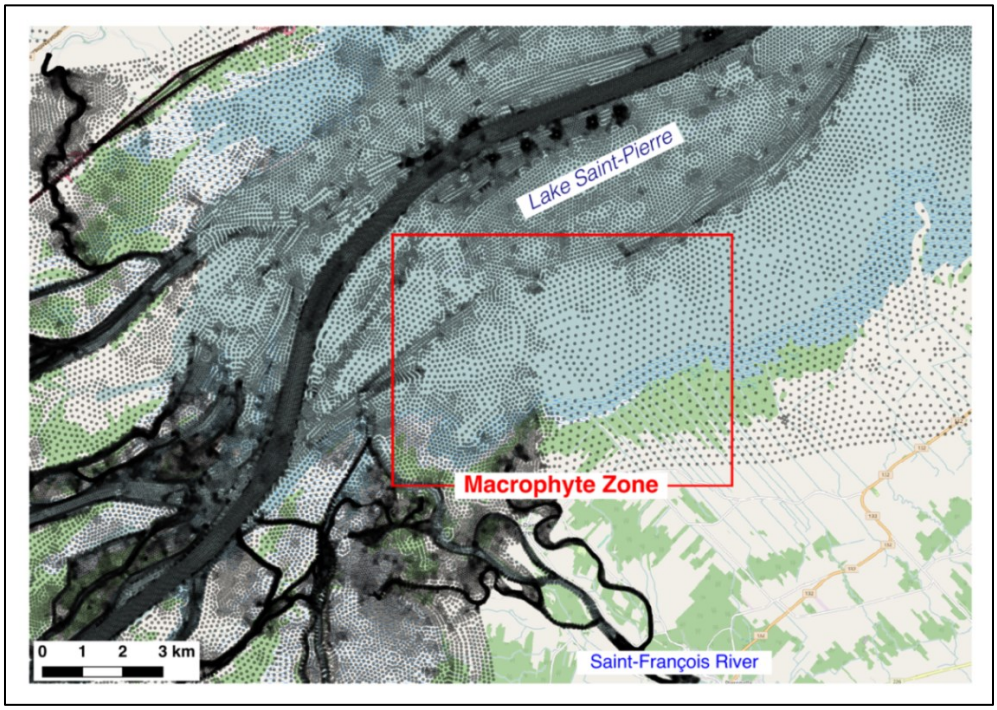

Figure 2.3. Variability in H2D2 grid resolution (black dots representing the center of grid cell) between the study zone and the river channels (the Saint-Francois River and the main navigational channel). The red rectangular represents the GRIL zone with field measurements taken between 2012 and 2017.

3. Research question

Considering the context of Lake Saint-Pierre and the current state of knowledge about flow-macrophyte interactions on the scale of entire open-channel water bodies, many questions remain unaddressed. In this project, I aim to answer the following research question: to what extent is the flow affected locally by the friction caused by abundant submerged vegetation in LSP at the mouth of the SFR during the months of July – September each year?

The study aims to fulfil two goals – 1) develop a three-dimensional hydrodynamic model of LSP including the Saint-François tributary for varied flow conditions, and 2) quantify the impact of aquatic plants on water flow at the mouth of the SFR using novel approaches.

4. Methodology

4.1 Three-dimensional model: Delft3D

The 3D model used in this study is Delft3D (D3D) from Deltares (version 4.01.01.rc.03). It can simulate flow dynamics in two and three dimensions and has the capacity to include sediment transport and the effect of macrophytes. D3D is open-source software and is commonly used for creating hydrodynamic models of fluvial, lacustrine and coastal / tidal environments. D3D is commonly a black-box solution, which has a graphic-user interface (GUI) which calls upon various modules (or tools) for building and running the model. Such tools are used to: generate regular curvilinear grids (RFGRID tool), generate depth and roughness coefficient maps (QUICKEN tool), export results as shapefiles through its own utility and display simulation results as maps or time series graphs (QUICKPLOT tool). Currently Deltares has launched its latest commercial version of Delft3D-FM (Flexible Mesh), which allows the use of irregular grids for complex channel shapes.

D3D is based on the Navier-Stokes and continuity equations, allowing simulations through either boundary-fitted sigma (σ) or equidistant Z coordinate layers. The available vertical grids have different applications depending on how steep the local bathymetry. The main difference between the available vertical grids is the number of available vertical layers – constant number for σ layers and varied for Z grid. The Z grid is not boundary fitted thus will be generated as a staircase (Figure 4.1).

Both steady and non-steady flow conditions can be simulated in D3D. When generating bathymetry from XYZ sample files (a simple text file with x, y, and z coordinates (termed as samples)), D3D offers two interpolation approaches: grid cell averaging and triangular

interpolation. The choice of the more efficient method depends on the depth point density. When there are more coordinate samples than the grid points, grid cell averaging is the most suitable approach. Otherwise triangular interpolation is preferred. However, triangular interpolation is markedly more time demanding.

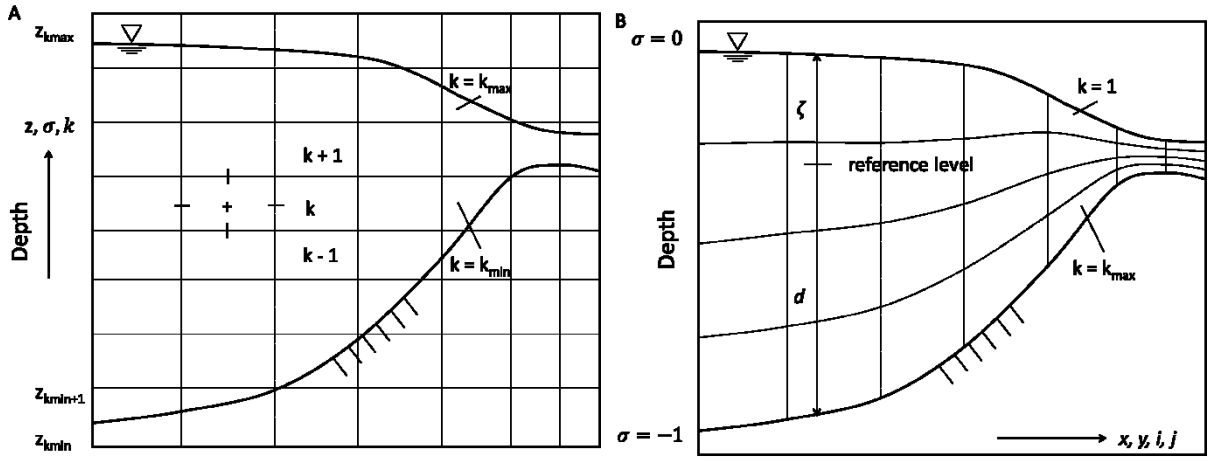

Figure 4.1. Schematic longitudinal profile with vertically exaggerated water surface for (a) Z-grid, and (b) sigma layers (reproduced from Delft3D-Flow user manual, 2014, p. 377).

A single grid can be locally refined, although this is done along the whole grid rows and/or columns (Figure 4.2A). To counteract unnecessary refinement along the whole rows and columns, D3D offers domain decomposition (Figure 4.2B), where multiple domains can share the same borders. The required data are passed automatically by D3D along connecting boundaries. If Delft3D-FM open source version is available (unconfirmed), it will be possible to use both regular and irregular grids in the same model to better accommodate the shape of LSP.

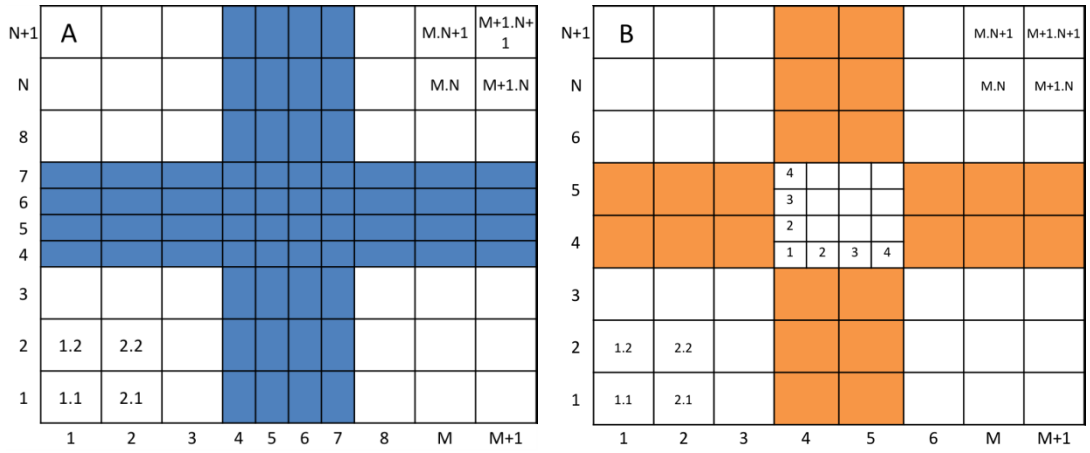

Figure 4.2. Single grid refinement (a) along the entire rows and columns in blue colour, and decomposed grid refinement (b) with a high-resolution second grid in the center of a coarser grid.

4.2 Domain Generation

4.2.1 Single Domain Grid Generation

The initial model of LSP used a single grid. It was generated in RFGRID tool (Delft3D utility used to generate model domains/grids). A land-water boundary file (a file that contains the outline of a water body) was required for this step and was generated by loading the lake boundary shapefile into QUICKPLOT and exporting it as a land-water boundary file. It allowed overlaying splines in different sections of the lake and generating grids from these splines. Since the lake has multiple channels, several segment grids were created and merged into one single grid in RFGRID. The upstream section of the lake represents the Sorel-Berthier archipelago, consisting of approximately 103 islands. Due to this complexity, a Cartesian rectangular grid (Figure 4.3) was preferred instead of a curvilinear channel shape grid. This approach avoided continuity problems (eventual drying up or overfilling of the modelled channel/water body) noted in test runs. In total the grid consists of 796 x 260 cells out of which only 140 133 (68%) are active elements. The average cell size is around 70 m.

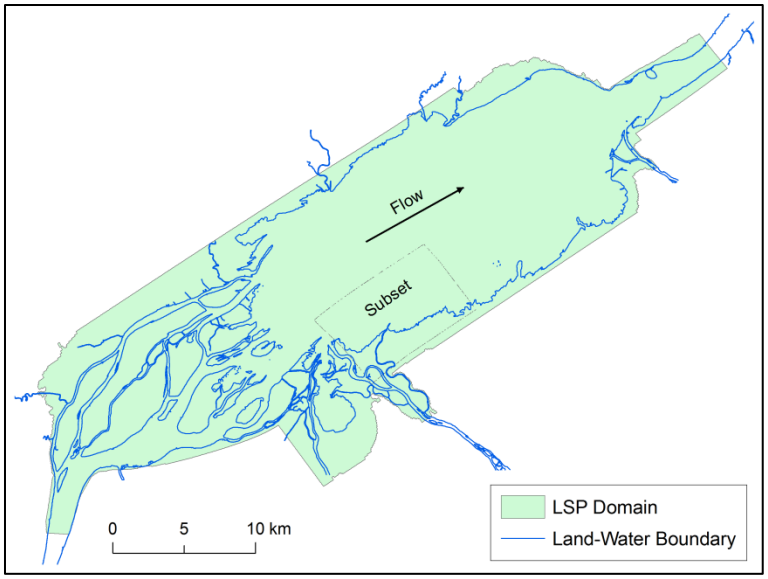

Figure 4.3. The designed Cartesian domain of the lake model.

4.2.2 Multi-domain Grid Generation

The grid generated for the single domain model was then used for the second multi-domain decomposed model. In order to focus on the area at the mouth of the Saint-François River (subset), two connected grids were required (Figure 4.3). A portion representing the area at the confluence of the Saint-François and Saint-Lawrence Rivers was extracted in RFGRID and saved as a separate grid. The number of active elements was decreased to 129,883, and the subgrid consisted of 375 x 246 cells and 92,250 active elements. The purpose of using several grids was to refine certain areas to obtain a smaller cell size. A sensitivity analysis was carried out to test different column-to-column and row-to-row ratios (1-to-1, 1-to-3, 1-to-5) between the subset and the surrounding grids (Figure 4.4). The differences in the minimum and mean depth-averaged velocities between different grids ratios are negligible. The maximum depth-averaged velocity decreased by less than 10% at 1-to-3 grid ratio (refined grid cell of around 25 m), thus avoiding the need to use a higher resolution subset grid (Biron et al., 2007), and

optimizing the time required to complete each run (55 min (1-to-1), 4 h 25 min (1-to-3), and 7 h 50 min (1-to-5) with 5 vertical layers in the subset grid at 0.1 min time step). Both grids were then connected through domain decomposition, in which boundary conditions data were indicated for the larger grid only. All required data to run the simulation within the refined area were transferred through the connecting boundaries between both grids, including 1246 grid nodes.

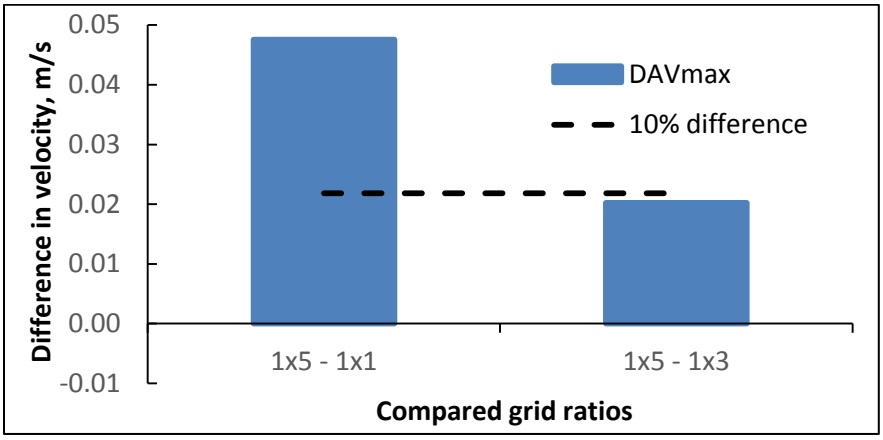

Figure 4.4. Grid sensitivity analysis. Difference in depth-averaged velocity (in blue (DAVmax) – maximum depth-averaged velocity) between compared ratios (1x1, 1x3, 1x5). The dashed line represents the 10% threshold difference.

4.3 Bathymetry

The model needs information on bed topography. D3D requires positive elevation values downwards for the bathymetry (Delft3D-FLOW, Manual), where datum is a known water level value or any other arbitrary elevation represented as a horizontal reference plane (Figure 4.5). A negative value in the generated depth indicates an elevation above the reference plane. The original DEM was thus converted into the appropriate D3D coordinate system by subtracting all elevation values from the highest elevation present in the original DEM (15.78 m) and multiplying by -1.

D3D does not accept conventionally used DEM files. A specific depth file needs to be created in QUICKEN, which will contain x, y, z points. Once both grid and xyz files are loaded into QUICKEN, depth files can be generated and exported. Initially the cell averaging approach was applied, followed by the "internal diffusion" command interpolating the elevation in the small blank areas. Once all grid cells contained elevation data, this was exported as DEP file (Figure 4.6).

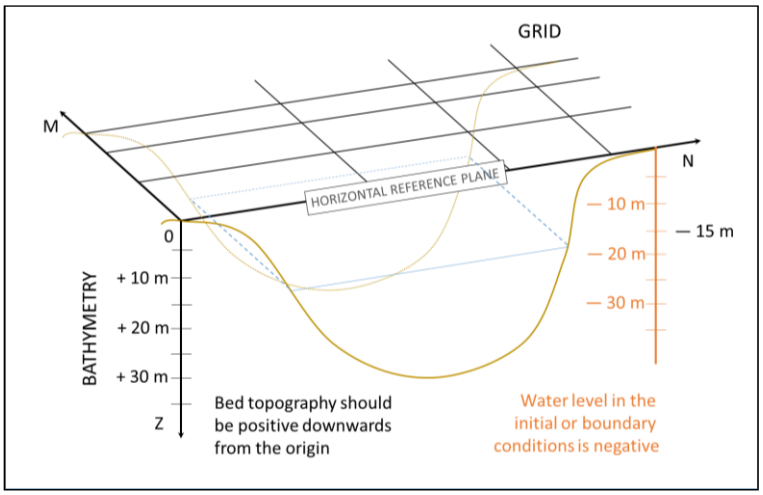

Figure 4.5. The coordinate system used in Delft3D for bathymetry and boundary conditions. Note the sign attribute in case of depth file generation (black Z vertical axis) and boundary conditions water level (orange vertical line)

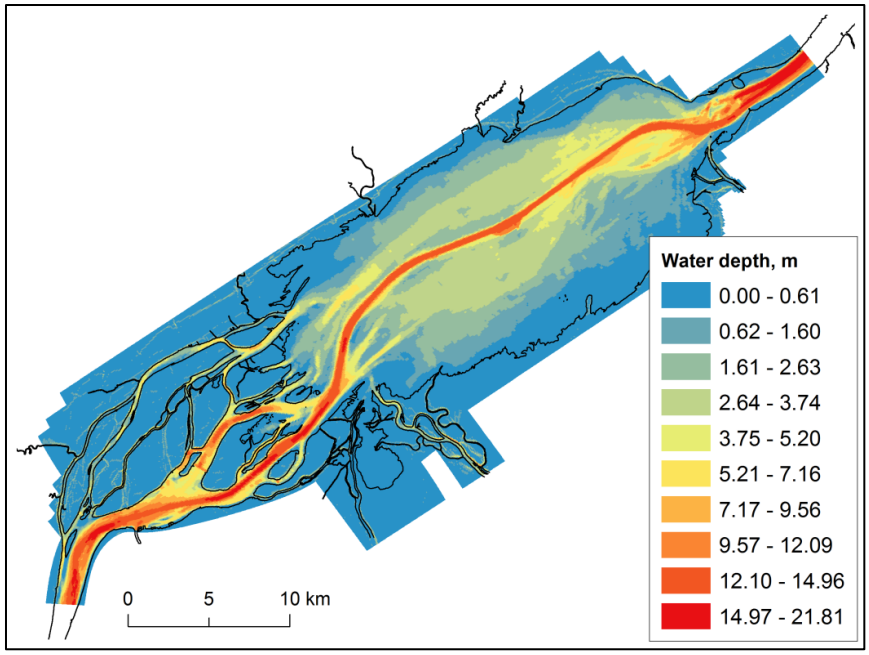

Figure 4.6. Water depth used in LSP models for low flow stage simulations (Q_{SLR} = 7990 m^3/s)

4.4 Manning's n maps

D3D allows for different options for the roughness coefficient (resistance to flow caused by bed and obstacles found in-channel). The simplest approach is to indicate a single value for the entire domain. To accurately simulate hydrodynamics in LSP, a roughness coefficient map was required (Figure 4.7). After the entire grid contained roughness coefficient values, the data was exported as a DEP file. Since D3D requires the roughness coefficient to be indicated in the u (streamwise) and v (lateral) directions regardless if the value is the same or not, some manual modifications were implemented in the exported file. Indeed, as the number of active elements is less than the total number of cells, D3D attributes a large negative number to inactive cells, which needs to be replaced with a positive number larger than 0 (a very small number was chosen). Failing to perform these modifications results in the model crashing. After the numbers were corrected, all values in the file were selected and copied at the end of the

document to provide required values in both the u and v directions, and saved with a new file extension *.rgh.

4.5 Model Preparation

After generating the required grid, depth and roughness coefficient map files, the actual model of LSP was assembled in the FLOW module of D3D. Table 4.1 summarizes the boundary conditions and other relevant data used in the models. The model was built, calibrated and tested using the June 18th 2012 data. August 19, 2012 and October 2, 2010 were used for water level validation.

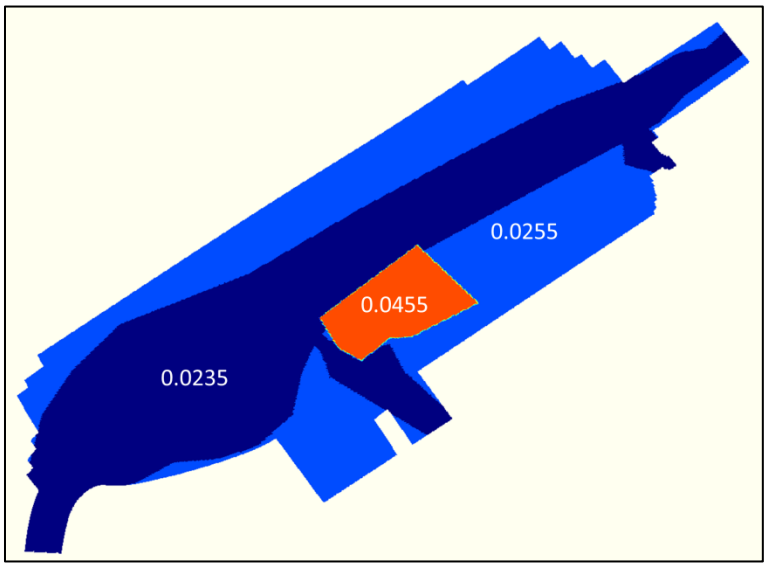

Figure 4.7. Manning's n spatial distribution after the calibration of LSP model. The area coloured in orange represents the study zone close to the confluence of the St-François and St. Lawrence Rivers.

Table 4.1. Boundary conditions used in models. Q stands for discharge, SLR – Saint Lawrence River, STF – Saint-François River

	2012/06/18	**2012/07/31-08/01**	**2012/08/19**	**2010/10/02**
Q_{SLR} (m^3/s)	7990	7480	7198	12400
Q_{STF} (m^3/s)	51	34	32.6	1150.8
Water $level_{SLR}$ (m) *	-12.4	-12.7	-12.6	-10.9
Water $level_{SLR}$ (m) **	3.37	3.09	3.23	4.88
Time step (*min*)	0.1			
Simulation period (*hrs*)	18			
Smoothing† time (*min*)	60			

* – Elevation converted to D3D datum, ** – the original elevation, † - required by the model to gradually transit from the initial conditions to the boundary conditions.

Depending on the grid orientation and the direction of simulated flow, the sign of the boundary conditions is positive if going from left to right or bottom to top and negative otherwise (Figure 4.8). Water level indicated in the boundary conditions needs to be negative (Figure 4.5).

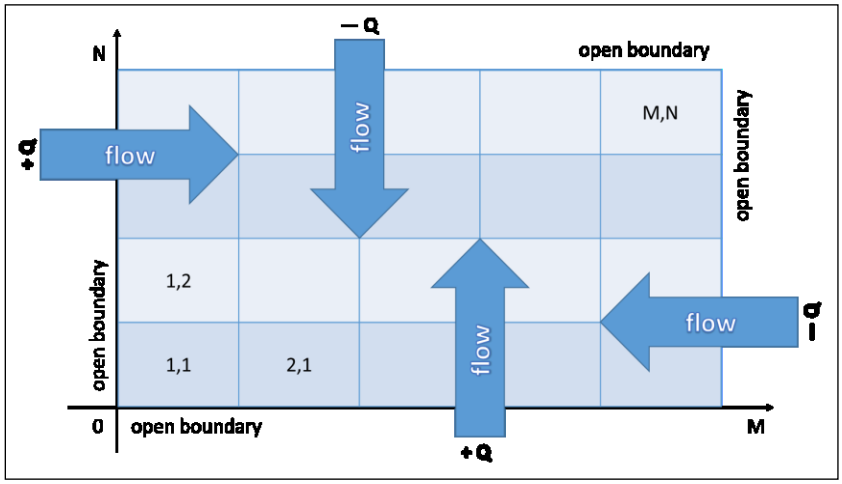

Figure 4.8. Sign attributes used in boundary conditions depending on the flow entry into the computational grid.

4.6 Calibration

The calibration was performed in two stages by adjusting Manning's *n* values throughout the entire domain using 18 June 2012 water level data. Since the first water level comparison revealed a large discrepancy between the simulated and measured values, Manning's *n* values were increased by 0.004. Following this, the value was progressively raised by multiple of 0.004, with a final value corresponding to an added 0.012, where the model overestimated considerably the water level (Figure 4.9). The comparison indicated that the simulated water level best approximated the measured ones with roughly 0.008 added, a few more simulation runs were performed testing for added values of 0.007 and 0.0075. Modification of the initial values by 0.0075 resulted in the closest approximation of the actual water levels (Table 4.2). Table 4.3 lists the friction coefficient initial and post-calibration values.

Table 4.2. Predicted and measured water level values at the gauging stations locations. Numbers indicate the adjustment of the initial Manning's n values.

Gauging Station	Measured, m	Simulated, m			
		Initial	Manning's n adjustment values		
			+ 0.007	+ 0.0075	+ 0.008
Sorel	3.98	3.71	3.96	3.98	4.00
Lake St-Pierre	3.61	3.50	3.60	3.61	3.62
Port St-François	3.41	3.37	3.39	3.39	3.39

Table 4.3. The initial and adjusted post-calibration Manning's n values.

Zone	Initial	Post-calibration
River channels	0.016	0.0235
Rest of the lake	0.018	0.0255
Study zone	0.035	0.0455

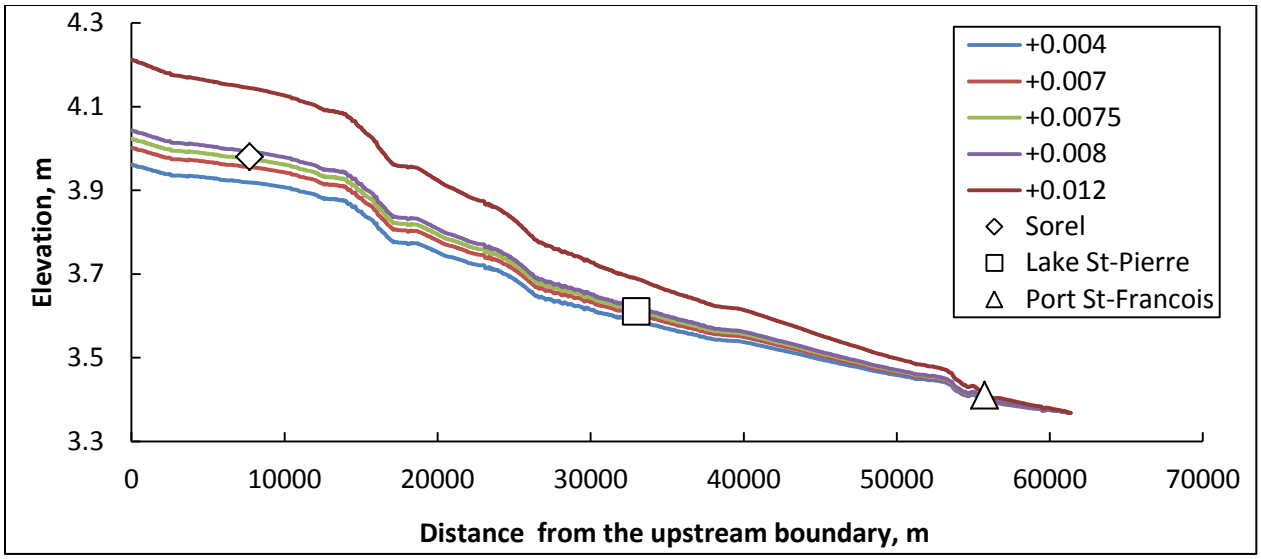

Figure 4.9. Simulated longitudinal water level profiles compared to the observed data from Sorel, LSP and Port St-François gauging stations. Each profile indicates the added value to the initial Manning's n values.

4.7 Validation

The models were validated using known water levels for flow conditions: August 19, 2012 (low flow) and October 2, 2010 (high flow). A difference within 5 cm between the simulated and observed water level is considered as acceptable. Table 6.3 summarizes the differences at three gauging stations located within the LSP area. For validation purposes two dates were simulated to represent the low and high flow stages. Almost all differences between simulated and measured water level fall within 5 cm apart from Sorel gauging station on October 2nd, 2010 (Table 6.3). The discrepancy at this location is 6 cm and taking into account the recorded high flow stage in comparison to the other simulated dates, this arguably remains within an acceptable level of error.

4.8 Macrophyte integration

The calibrated and validated models include submerged vegetation through a simple procedure based on varying Manning's *n* values. In the latest versions of D3D additional functionality is included to address the integration of the friction due to the presence of bed forms and submerged vegetation. Depending on the required type of simulation (2D or 3D), Delft3D includes vegetation using either trachytope function #154 (from Greek word τραχυτης meaning roughness), or a combination of bed resistance formulations in a modified 3D *k-ε* turbulence closure model, where *k* represents the turbulent kinetic energy and *ε* the turbulent kinetic energy dissipation rate (Delft3D-Flow user manual, 2014).

4.8.1 Trachytope Approach

This approach, applicable only in two-dimensional simulations, defines resistance and bed roughness on a sub-grid scale (allowing for several values per cell) through different resistance classes referred to as trachytopes. Application of a certain resistance class is implemented by inputting required parameters in the FLOW module and connecting specific text files, which need to be generated separately through manual editing. At each requested time step trachytopes are converted into a corresponding roughness coefficient (Manning, Chézy, or White-Colebrook). To cut the computational time, the user can change the time step required for calculation of roughness using trachytope functionality. These calculations could be executed every second time step, etc. Generally, all trachytope classes in D3D are separated into three broad categories: area, linear, and point, out of which area-type trachytopes are the most dominant as they could cover the entire model domain or subdomain. Linear trachytope

classes are suitable for simulation of linear features such as hedges or similar features. Each trachytope class has a specific number in D3D, and trachytope class 154 will be used in this project. This resistance class is based on the Baptist (2005) vegetation model. The required parameters are vegetation height h_v, plant density per unit area A, drag coefficient C_D and alluvial bed roughness C_b (Delft3D-Flow manual, 2014). The full contextual description of the approach is explained in the Delft3D-Flow manual (2014, pp. 269-270).

Additionally, the use of trachytope 154 resistance class requires 2 files: vegetation definition file, which lists vegetation types (type number, trachytope class number, related h_v, A, C_D, C_b), and the area file indicating proportion occupied by corresponding types in a grid cell. The ability of specifying proportions of cells occupied by several plant types differentiates this approach from the conventionally used Manning's n. The models which incorporate macrophytes through Manning's n have a single roughness value per cell and using coarser grid resolution over-generalizes the actual bed roughness and flow resistance locally. Furthermore, the adjustment of drag affects local shear stress, which in its turn impacts sediment transport simulation (Delft3D-Flow manual, 2014). The trachytope approach can thus provide reasonable and quantitatively accurate results within a 2D modelling framework, which from a practical perspective also reduces simulation time.

4.8.2 Three-dimensional vegetation model

D3D also offers a modified k-ε turbulence closure model, where plants are represented as rigid cylinders of a certain height (Fischer-Antze et al., 2001). The main input parameters in the corresponding equations (see Delft3D-Flow manual, 2014, pp. 273-274) are plant number per

unit area and stem width. The impact of vegetation on the flow is given through vertical distribution of the friction force affected by stems. Additional parameters such as the overall turbulence length scale C_l between stems, height, stem diameter, number of stems in a plant, and C_d coefficient need to be indicated in a text file with *.pla extension. The information on the number of plants/m^2 is also needed. This can be done by assuming an average number or by including a polygon file delineating the areas covered by the vegetation type. The *.pla file similarly can include data on several vegetation types and a defined time step (which can be different from the model time step). The full contextual description of the approach is described in the Flow manual (Delft3D-Flow user manual, 2014, pp. 273-274).

5. Comparison of two approaches of macrophyte simulation

5.1 Introduction

D3D has several approaches of simulating the presence of submerged vegetation in models – trachytope function #154 applicable in 2D simulations and modified 3D *k-ε* turbulence closure model suitable for 2D and 3D simulations. Unlike the conventionally used *k-ε* turbulence models in CFD, the modified 3D *k-ε* model implemented by Deltares includes the effect of vegetation on vertical mixing reproduced by the additional source terms in both the kinetic turbulent energy (*k*) and epsilon (*ε*) equations. The source term in *k* equation represents the work expended on fluid and is based on the vertical distribution of friction force, which accounts for plant geometry such as the stem height and width. The source term in *ε* equation considers the dissipation time of free turbulence in conjunction with the dissipation time scale of eddies in between the modelled macrophytes and limited by the smallest distance between plants (Delft3D-Flow user manual, 2014).

For large-scale studies, it is hypothesized that the trachytope function would be preferable since computational time is reduced in 2D simulations. From efficiency perspective, choosing a simpler approach for large models is valid and reasonable despite the availability of recent advances in computer technologies allowing more complex 3D simulations to be run.

To compare the trachytope function and modified *k-ε* turbulence model, the experimental study of Murphy et al. (2007) was chosen as methods and results are sufficiently detailed to build a D3D model and compare simulated and measured velocities. Indeed, the authors report all the essential parameters required for similar representation of macrophytes in D3D such as density and form, stem width and height. Furthermore, thesimple flume

configuration was straightforward to implement in D3D. This allowed proper testing of the trachytope function and modified 3D *k-ε* turbulence model in a simpler smaller model before applying the chosen method to the larger, more complex LSP model.

5.2 Methodology

5.2.1 Experimental design in Murphy et al. (2007)

Experimental runs were carried out in a glass flume with the following dimensions: 24 m (length) x 0.38 m (width) x 0.58 m (depth) with recirculating water (Figure 5.1). To provide unidirectional flow and eliminate turbulence and swirl, a 50-cm long array of wooden dowels coupled with rubberized mats followed by a 1-m honeycomb were installed at the inlet. The slope of the flume bed was kept constant at zero. Macrophytes were represented as rigid cylinders with an average diameter of 6 mm spaced out randomly on Plexiglas boards having two heights in different runs – 7 and 14 cm (Figure 5.1). Murphy et al. (2007) carried out 24 experiments, including 7 runs where velocity was measured by acoustic Doppler velocimeter (ADV) and 17 runs where velocity was measured by a two-dimensional laser Doppler velocimeter (LDV) (Table 5.1)

Out of 24 experiments, the results from run H were chosen for comparison with predictions using the trachytope function and modified 3D *k-ε* turbulence model, based on the largest reported discharge (1.43 cm^3/s) and cylinder height (14 cm) (Table 5.1). Murphy et al. (2007) measured average velocity in two zones defined as slow (bottom) and fast (top) zones, respectively. The border between these two zones is defined by the height of cylinders used in

the experiment run (14 cm for run H). The measured average velocity for run H was reported as 3.3 cm/s for the cylinder zone (slow zone) and 11.1 cm/s for the fast zone (Table 5.1).

Table 5.1. Summary of experimental conditions from Murphy et al. (2007).

Run	$Q \times 10^{-2}$ cm^3 s^{-1}	h, cm	H, cm	a, cm^{-1}	$S \times 10^5$	U_1, cm s^{-1}	U_2 cm s^{-1}	ΔU cm s^{-1}	β_1	$h - z_1$, cm	$Re_H \times 10^{-4}$
A	48	14.0	46.7	0.025	0.99	1.6	3.7	3.2	0.67	12.7	1.5
C	74	14.0	46.7	0.034	2.50	2.0	5.5	4.9	0.71	10.9	2.1
D	48	14.0	46.7	0.034	1.20	1.4	3.8	3.5	0.67	12.3	1.4
E	143	14.0	46.7	0.040	7.50	4.2	10.6	9.5	0.68	11.6	4.1
G	48	14.0	46.7	0.040	1.30	1.4	3.7	3.3	0.69	10.3	1.4
H	143	14.0	46.7	0.080	10.00	3.3	11.1	11	0.71	11.2	4.1
I	94	14.0	46.7	0.080	3.40	2.1	7.2	7.4	0.69	9.8	2.7
A6	17	7.0	29.8	0.025	0.30	0.6	1.6	1.6	0.64	5.8	0.4
B6	94	7.0	29.8	0.025	8.04	3.3	8.4	7.0	0.73	7.0	2.2
C6	48	7.0	29.8	0.025	2.42	1.7	4.4	3.7	0.70	3.4	1.1
A1	17	7.0	23.6	0.025	1.06	0.7	1.6	1.4	0.68	7.0	0.3
B1	94	7.0	23.6	0.025	11.57	4.3	10.2	9.1	0.65	7.0	2.0
C1	48	7.0	23.6	0.025	4.27	2.2	5.1	4.8	0.61	5.1	1.0
A2	17	7.0	14.0	0.025	1.73	1.3	2.9	2.4	0.67	7.0	0.3
B2	94	7.0	14.0	0.025	48.66	7.8	15.5	11.8	0.65	7.0	1.7
C2	48	7.0	14.0	0.025	30.05	5.0	10.6	7.8	0.72	7.0	1.1
A3	17	7.0	10.5	0.025	12.44	2.5	5.4	5.0	0.59	2.9	0.4
C3	48	7.0	10.5	0.025	66.61	6.9	14.7	11.0	0.71	7.0	1.0
A5	17	7.0	8.8	0.025	28.35	2.8	5.3	3.2	0.77	3.9	0.3
C5	48	7.0	8.8	0.025	134.04	9.9	18.7	12.6	0.70	7.0	1.1
C6D	48	7.0	29.8	0.080	2.03	0.8	4.6	5.3	0.72	7.0	1.1
C2D	48	7.0	14.0	0.080	36.64	3.0	9.3	9.5	0.66	7.0	0.9
A2D	17	7.0	14.0	0.080	4.74	1.0	3.4	3.4	0.70	5.3	0.3
A3D	17	7.0	10.5	0.080	23.19	2.0	5.2	4.6	0.71	5.4	0.3

Q – discharge at inlet, h – height of cylinders, H – total water depth, a - is the projected frontal area of the vegetation per unit volume, S – measured slope, U_1 – mean velocity in the vegetated layer (near the flume bottom), U_2 – mean velocity in the non-vegetated layer (near the surface), ΔU – the total velocity difference in a profile, β - fraction of the difference between U_2 and U_1 over ΔU, $h–z_1$ – vortex penetration distance, Re_H – Reynold's number.

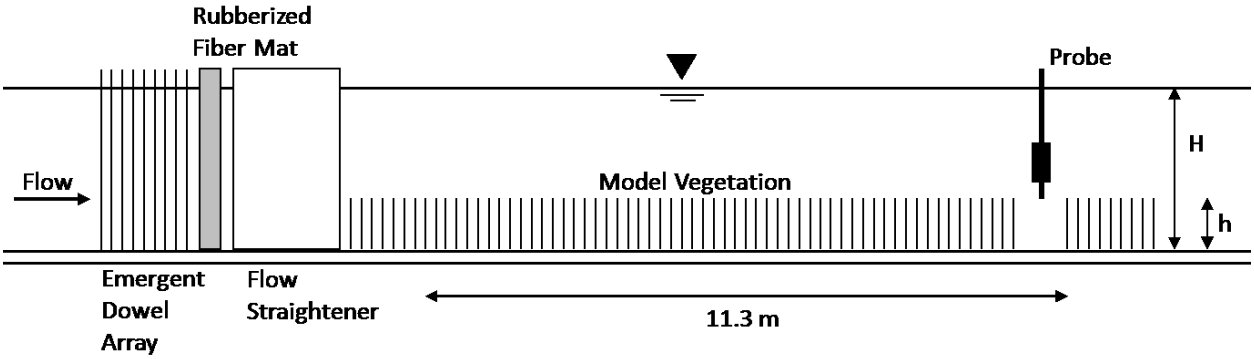

Figure 5.1. Experimental design as described in Murphy et al. 2007 (adapted from Murphy et al., 2007, Figure 2a)

Table 5.2. Boundary conditions and vertical layer distribution for D3D runs.

Run	Discharge at inlet, m^3/s	Water level at outlet, m	Manning's n	# of layers	% of total depth per layer	Macrophyte simulation
1	1.43×10^{-6}	0.467	0.01	1	100	–
2				5	20	–
3				10	10	Yes (K/E)
4				20	10 x 7	Yes (K/E)
					10 x 3	
5				1	100	Yes (T)

* K/E – modified 3D *k-ε* turbulence model, T – trachytope function.

5.2.2 Delft3D simulations

Five steady flow simulations were carried out in Delft3D in which vertical layers and cylinders were added step-wise starting from a single vertical layer to 20 layers (Table 5.2). The boundary conditions as well as Manning's n coefficient were kept constant throughout all simulations runs. Manning's n value of 0.01 was used for glass flume bed according to the values for artificially lined channels indicated by Munson et al. (2009, p. 549), which do not account for the presence of rigid cylinders (vegetation) in the modelled flume. This allowed isolating the predicted effect of cylinders on flow by the tested approaches. The mesh representing the flume consisted of 240 x 8 cells, and 1920 active grid elements. The model design used a similar approach as previously described and the procedure did not bear significant changes in generation of the mesh. Eight equally spaced rows in Y direction (4.75 cm distance between the grid lines), and 240 columns in X direction spaced every 10 cm were delineated, which resulted in 10 x 4.75 cm grid resolution. Bathymetry was designed to replicate the flume tank bed – with a zero-bed slope. All tests counted 6 hours of computational time including 1 hour of smoothing time (period of gradual transition between

the initial and the boundary conditions to allow time for the model to reach stable state and dissipate energy oscillations at the beginning of a simulation) at time step of 0.01 minute. To approximate the presence of wooden dowels, rubberized mats and honeycomb from the experiment, 7 thin dams (lines that restrict lateral flow) were put parallel to the model walls in D3D model before the delineated macrophyte zone.

The relationship between the total exposed area of cylinders, a, and number of plants is the following (White et al., 2004):

$$a = md, \quad (1)$$

where a is total cylinder area exposed to the flow, m is cylinder density per unit area [# cylinders/m^2], d is stem diameter. Murphy et al. (2007) report a total exposed area of cylinders value of $a = 0.08\ cm^{-1}$ or $8\ m^{-1}$ (Eq. 1), requiring modification of D3D vegetation definition files for testing. Therefore, the total number of cylinders as reported is:

$$m = a \div d = 8\ m^{-1} \div 0.006\ m = 1333\ m^{-2} \quad (2)$$

The trachytope function requires $8\ m^{-1}$, whereas the modified 3D k-ε model requires $1333\ m^{-2}$ in their plant definition files.

5.3 Results

Model run 1:

The purpose of this run is to estimate the stability and behaviour of the created Delft3D model. A single vertical layer was tested and spatially homogenous flow is expected throughout the domain. The flow field simulated by Delft3D is indeed stable, with a constant depth-

averaged velocity for the entire domain of 8.06 cm/s (Figure 5.2A). No acceleration or deceleration is observed in any part of the domain.

Model run 2:

This run builds upon the previous run, with 5 depth layers (20% of depth each). Similarly, no macrophyte submodel was used in this run. The range of the predicted depth-averaged velocity remains comparable to run 1, i.e. 8.06-8.43 cm/s (Figure 5.2B), and is somewhat constant throughout the whole domain. The mean velocity is calculated by averaging velocity values at 20% and 80% depth (layers 2 and 4 from top to bottom). Although the range of the average velocity throughout the modelled flume is larger than in run 1, it can be considered relatively homogenous and uniform in comparison to runs 3 and 4, which display the largest variation in velocity spatially and vertically.

Model run 3:

The purpose of this simulation is to increase velocity point sampling vertically, with 10 equally-spaced vertical layers, thus covering 10% of the depth per layer. Macrophytes were incorporated using the modified 3D k-ε turbulence model. The depth-averaged velocity was calculated by averaging velocity for layers 3, 4, 7 and 8 (top to bottom). Velocity profiles were derived for maximum, width-averaged and minimum flow at the cross-section indicated by the black line in Figure 5.2C. The introduction of the submerged vegetation increased the range between the minimum and maximum velocity predicted: from U = 3.1 to 14.1 cm/s (Figure 5.2C). It is worth noticing the appearance of

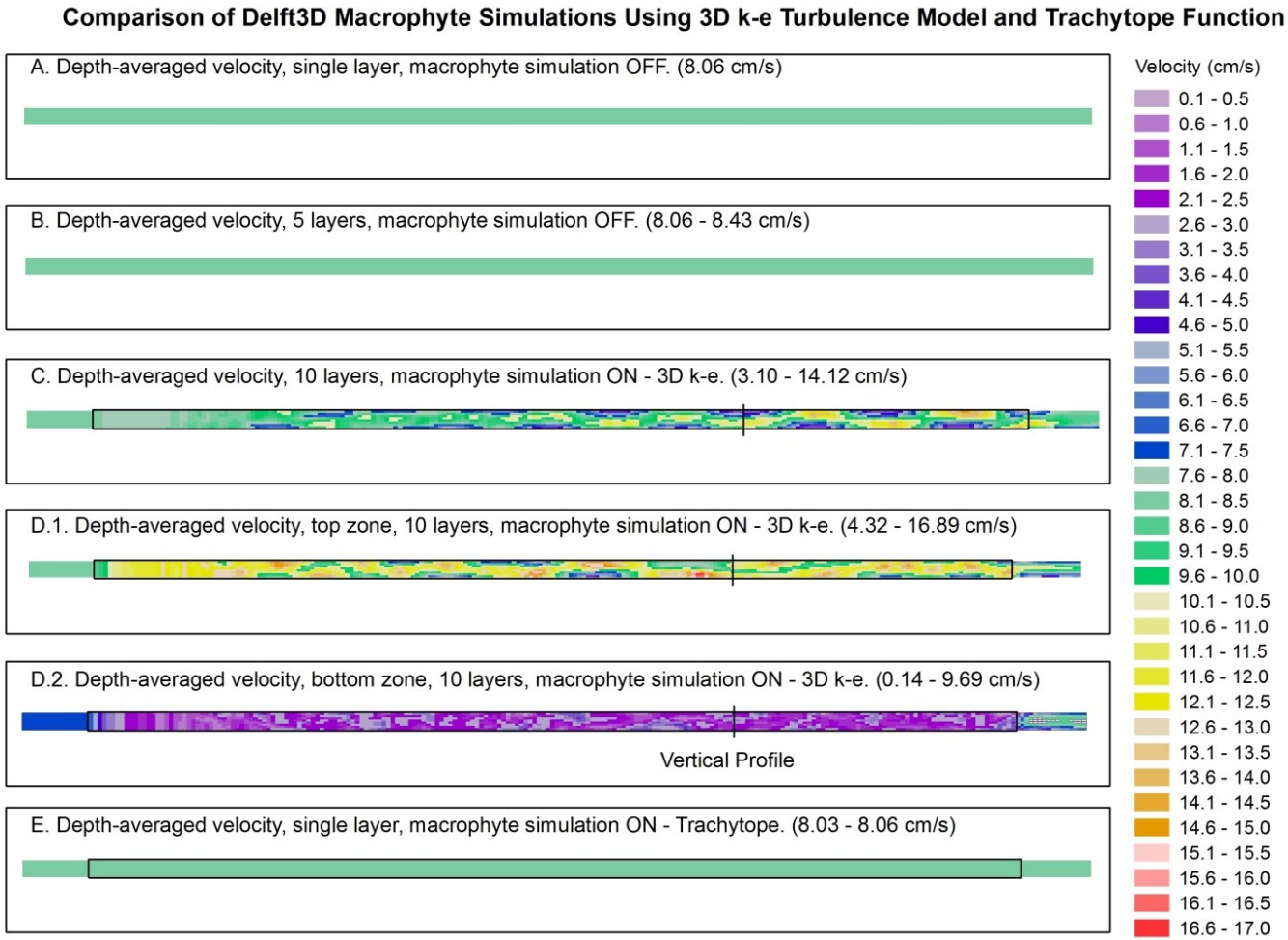

Figure 5.2. Spatial variation of depth averaged velocity in the rectangular shaped model – without cylinders - (A) single depth layer, (B) 5 depth layers, with cylinders (C) 10 depth layers, (D1, 2) two zones, 20 layers, and trachytope function (E) single depth layer. Black rectangular represents the modelled macrophyte zone. Black line indicates the position of the vertical profiles and time series graphs. Water is flowing from left to right.

meandering trend in the zone of macrophyte simulation, as well an overall decrease in velocity upon entering the macrophyte zone.

Model run 4:

This run approximates most the experimental setup described in Murphy et al. (2007). Two zones have been designed each having 10 layers (so 20 layers in total). Since in the experimental design, the height of cylinders reaches ~30% of the total depth, each layer in the slow zone represents 3%, and respectively 7% in the fast zone. This allows for a comparison between vertical velocity profiles from Murphy et al. (2007) (Figure 5.3A) and from D3D predictions (Figure 5.3B, C). Similarly to run 3, profiles were derived for maximum, width-averaged and minimum flow (Figure 5.3C). Having 20 layers allowed deriving smoother vertical velocity profiles in the indicated cross section (Figure 5.2 D.1 & D.2). Both vertical zones displayed the same meandering trend observed in run 3 (Figure 5.2 D.1 & D.2). The mean velocity for the modelled macrophyte zone was 2.2 cm/s in the slow zone at the bottom of the flume, and 11.0 cm/s in the faster zone, which are close to the measured values, although slightly underestimated (Table 5.1). From Figure 5.2 D.2 it is apparent the flow is restricted in the slow zone passing through numerous cylinders. The faster zone shows an increase of velocity near the surface which is unobstructed by the incorporated vegetation.

Since the results of runs 3 and 4 displayed large velocity variation length- and width-wise in the model, velocity profiles were computed for maximum, width-averaged and minimum velocity (Figure 5.3B, C). The original figure (Figure 5.3A) presented in the research paper by Murphy et al. (2007) does not display the topmost part of velocity profile (missing 7 cm), only 9 layers (Figure 5.3B) and 18 layers (Figure 5.3C) were presented in the figure. The velocity

profiles show a relatively good match between the predictions taken at the cross section and the measured values by Murphy et al. (2007) (Figure 5.3A). In the experimental results, where detailed vertical velocity measurements were taken at small increments of 0.5 cm, transition between the slow and fast zones is relatively smooth (Figure 5.3A). Using 10 layers in the D3D model results in a more abrupt transition (run 3, Figure 5.3B), which nevertheless represents correspondingly the experimental vertical profiles (Figure 5A). With 20 vertical layers in two zones (run 4), the same pattern is observed, although with smoother transition between the slow and fast zones (Figure 5.3C).

Model run 5:

In this run macrophytes were modelled using the built-in trachytope function #154. Since this function is applicable only in two-dimensional simulations a single vertical layer was used. It was expected that the model would produce a slower depth-averaged velocity in the macrophyte zone compared to runs 1 and 2. Figure 5.2E reveals that this is not the case. The predicted depth-averaged velocity in run 5 is similar to run 1 (without macrophyte simulation) ranging from 8.03 to 8.06 cm/s, which undermines the applicability of the trachytope approach for further testing in the LSP model.

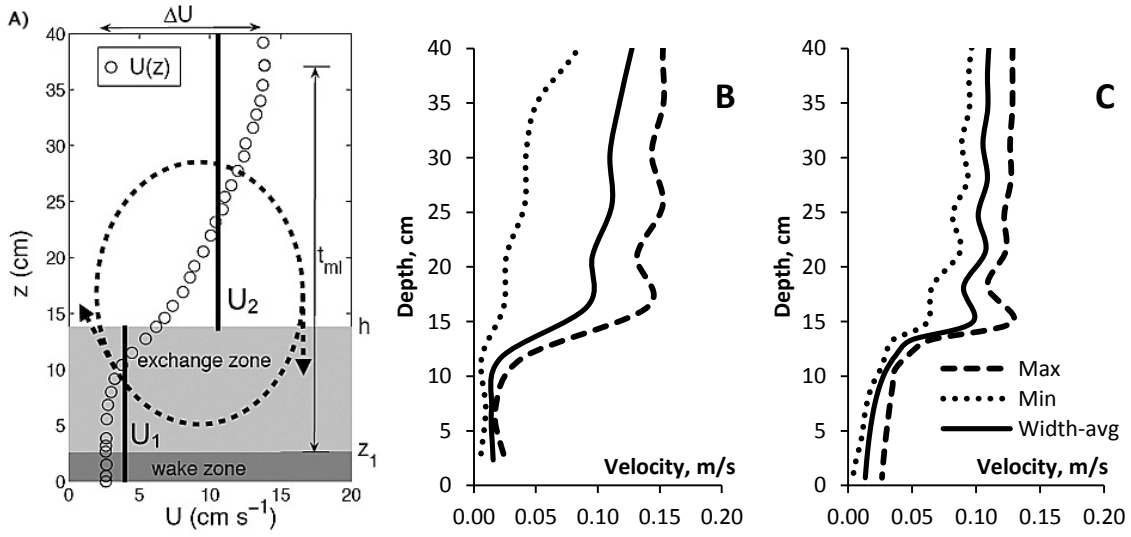

Figure 5.3. Vertical velocity profile for (A) experimental measurements (Murphy et al., 2007), (B) a single 10-layer zone simulation (run 3), and (C) 20-layer simulation (run 4). Dotted line represents the minimum velocity, solid line – width-averaged velocity, and dashed line – maximum velocity in the cross-section. Macrophytes are incorporated using 3D *k-ε* turbulence model. The experimental measurements do not include the topmost 7 cm of the depth due to ADV sampling distance; the open circles are extrapolated by the authors. D3D profiles exclude the topmost layer (B), and two topmost layers (C).

5.4 Discussion

The most important observation derived from the estimated results is the minimal effect on the flow field by using the trachytope function #154 (simulation run 5, Figure 5.2E) in comparison to the predictions resulting from the modified 3D *k-ε* turbulence model (simulations 3 and 4). The results of this comparison highlight the advantage of using 3D modelling over 2D modelling approach, providing more insight as to what happens along the flow path as well throughout the water column. Knowledge of predicted velocity at different depths could provide additional insight into mean water residence time.

While comparing the performance of the trachytope function #154 versus the modified 3D *k-ε* model, simulation runs 3 and 4 as opposed to run 5 displayed larger variation of mean velocity in the macrophyte zone. In both runs, the flow tends to meander once entering the

simulated macrophyte zone, which could be attributed to significant increase in drag. To counteract the appearance of the meandering flow thin dams were used in the model, as this is a built-in functionality in Delft3D. Their incorporation into the model attempted to replicate the approach used in the experimental design in immediate vicinity of the inlet. Thin dams represented thin impermeable walls parallel to the flume walls and were expected to straighten the flow before entering the macrophyte zone. The tests showed this approach to be irrelevant for this purpose. Meandering trend reappeared slightly further downstream. Water level and velocity consistently oscillate throughout the whole simulation at the observation point (Figure5.4A and B). Although there is oscillation observed in water level, the changes are minor around 46.97 cm value with delta z = ± 0.005 cm. Velocities ranged between 8 and 10 cm/s. Running these models with the tested 250 cylinders/m^2 density (instead of 1333 cylinders/m^2) removes the meandering trend in both models and stabilizes the flow (as seen from the times-series observation, Figure 5.4A and B. Overall, the flow correctly slows down in the slow zone and increases in the fast zone.

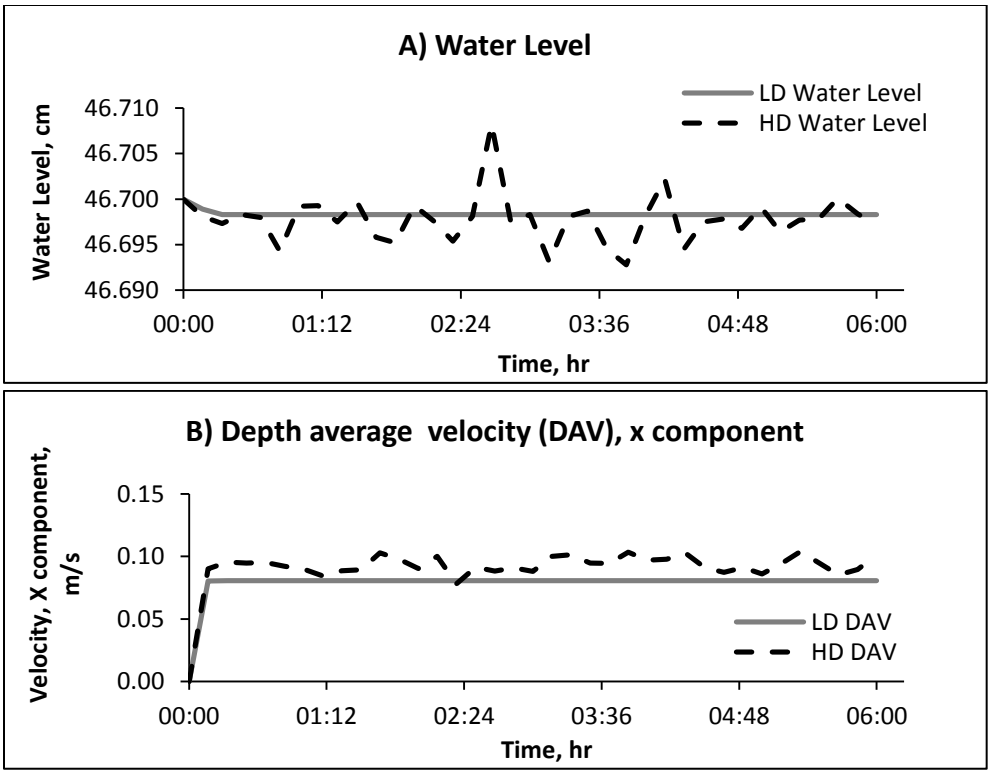

Figure 5.4. Time series results for A – water level, and B – depth averaged velocity (DAV, x component). LD – low density cylinder simulation (250 cylinders/m^2), HD – high density cylinder simulation (1333 cylinders/m^2).

To get additional insight into how D3D model behaves at different depths, vertical profiles were computed for runs 3 and 4. As expected, doubling the number of vertical layers produces smoother profiles and facilitates flow comparison between the experiment and simulations. Although run 3 has half as many sampling points it follows the same trend observed in run 4. An interesting feature is observed at roughly 15-20% depth from the bottom. It differs from what was measured in the flume by Murphy et al. (2007), where the flow tends to be constant at around 3 cm/s. In both runs, the flow displays a slight deceleration at this point as calculated by D3D, which is difficult to understand. Otherwise, as judged qualitatively by vertical profiles of the width-averaged velocity, D3D simulates very well the Murphy et al. (2007) laboratory run H. Similar good agreement between experimental data and the modified *k-ε* model predictions

was observed by Fischer-Antze et al. (2001) who conducted a series of tests attempting to replicate results of flume studies of Tsujimoto et al. (1991), Pasche (1984), and Lopez and Garcia (1997). The successful comparison of Fischer-Antze et al. (2001) results led them to conclude that the *k-ε* model approach could be applied to large scale river reaches.

Based on the comparative tests with Murphy et al. (2007) experimental results, it was decided to not use the trachytope function in this study. The modified 3D *k-ε* turbulence model is clearly more suitable for further study of the impact on the flow by the simulated submerged vegetation in the LSP model. Although the use of three-dimensional modelling increases the computational time and requires more powerful computers in general, this is deemed necessary to properly simulate the impact of macrophytes on theflow field in LSP.

6. A 3D numerical model investigation of the impact of macrophytes on flow dynamics in a large fluvial lake

This chapter was written in collaboration with my supervisors Dr. Pascale Biron and Dr. Jay Lacey, as well as Morgan Botrel, Dr. Christiane Hudon and Dr. Roxane Maranger. The manuscript will be submitted to *Freshwater Biology*.

As first author I was responsible for the development of methodology, collecting the data, model creation, calibration and validation, presentation of results, statistical analyses and writing of the manuscript. Dr. Pascale Biron provided guidance for all stages of the research and writing process as well as contributing important revisions in response to the constructive criticism from co-authors of earlier versions of the manuscript. Dr. Jay Lacey contributed major revisions and suggestions for the manuscript. Morgan Botrel, Dr. Christiane Hudon and Dr. Roxane Maranger were responsible for the field campaign that took place in LSP between 2012 and 2017. This allowed testing the model using an exceptionally detailed and unique field dataset. They also offered their expertise on submerged aquatic vegetation and commentaries on the manuscript.

Author names and affiliations

M. Bulat[a,b], P. M. Biron[a,b], R.W.J. Lacey[b,c], M. Botrel[b,d], C. Hudon[b,e], R. Maranger[b,d]

[a] Department of Geography, Planning and Environment, Concordia University, Montréal, Québec, Canada

[b] Groupe de Recherche Interuniversitaire en Limnologie (GRIL)

[c] Département de génie civil, Université de Sherbrooke, Sherbrooke, Québec, Canada

[d] Département de biologie, Université de Montréal, Québec, Canada

[e] Environment and Climate Change Canada, Montréal, Québec, Canada

Corresponding author

Department of Geography, Planning and Environment, Concordia University, 1455 De Maisonneuve Blvd. W., Montréal, Québec, Canada, H3G 1M8 (M. Bulat), contact@maximbulat.com

Abstract

1. Aquatic plants (macrophytes) are known to affect flow dynamics, contributing to flow resistance. Most studies on flow-vegetation interactions are performed in laboratory flumes and focus on the flow field around plants, with little research at the level of vegetation patches in large aquatic ecosystems. In most hydrodynamic models, increased drag due to plants is modelled by increasing the Manning's *n* roughness coefficient.

2. The objectives of this study were to: 1) develop a 3D hydrodynamic model (Delft3D) applicable to large water bodies including a novel approach to represent macrophyte resistance (modified 3D *k-ε* turbulence closure model), and 2) compare the modelled flow with field measurements for different vegetation configurations and patch arrangements. Work was

carried out in Lake Saint-Pierre (LSP), a large fluvial lake of the St. Lawrence River in Québec, Canada.

3. Results showed a marked increase in residence time in the zone affected by macrophytes when using the modified *k-ε* turbulence closure model compared to the Manning's *n* approach, particularly near the bed. An improved agreement with field measured depth-averaged velocity is obtained with this novel approach (correlation coefficient of 0.80 compared to 0.46 with Manning's *n* only). In addition, a good fit was obtained between vertical velocity profiles modelled and measured in the macrophyte zone. Sensitivity analysis revealed that the additional drag due to plants was closely associated with plant height, but that plant density played only a minor role in retarding velocities.

4. These findings indicate that it is possible to accurately quantify both the horizontal and vertical flow modulations resulting from submerged vegetation in large fluvial systems.

Keywords

Lake Saint-Pierre, Residence time, Hydrodynamics, Ecological services

6.1. Introduction

Submerged aquatic vegetation (SAV) is a vital component of aquatic ecosystems and provides many critical ecosystem services (Carpenter and Lodge, 1986; Jeppesen et al. 1997). Indeed, macrophyte patches create spawning and rearing habitats and serve as a source of diversified food for fish populations (Thomaz et al. 2008), wintering water birds (Schmieder et al. 2006), and also provide protection from predators (Grenouillet et al. 2001; Katayama, 2014). The presence of macrophytes fosters aquatic invertebrates and zooplankton richness and

biomass (Rennie and Jackson, 2005; Bolduc et al. 2016). SAV however may also markedly reduce water velocities (Boudreau et al. 1994; Morin et al. 2000b; 2003; Marjoribanks et al. 2014; 2017), which in turn can influence major biogeochemical cycles (Bal et al. 2010). By facilitating sedimentation and increasing water residence time, SAV can enhance nutrient/metal processing and removal (e.g. Madsen et al. 2001; Maine et al. 2006; Costa et al. 2018). Quantifying the impact of macrophytes on flow dynamics is thus essential to estimate elemental fluxes and model nutrient budgets in rivers and lakes (Janse, 1997; Billen et al. 2001; Justić et al. 2002; Garnier et al. 2005; Hudon and Carignan, 2008; Tall et al. 2011).

In situ studies estimating the impact of vegetation on flow dynamics in aquatic ecosystems are rare, particularly at larger spatial scales. Indeed, most laboratory studies have used a simplified representation of plants using various types of materials to assess their potential impact on hydrodynamics (Fischer-Antze et al. 2001; Sharpe and James, 2006; Murphy et al. 2007, Kubrak et al. 2008). The use of rigid cylinders to simulate plants is very common, with only a few studies representing plants as flexible strips (Kubrak et al. 2008, Dijkstra and Uittenbogaard, 2010) or as a complex three-dimensional (3D) point cloud (Boothroyd et al. 2017). Some laboratory experiments have attempted to replicate the natural complexity of macrophytes by emulating different patterns (linear, random, staggered arrays of cylinders) (Murphy et al. 2007; Kubrak et al. 2008; Yang 2008). Nevertheless, these laboratory experiments remain simplistic as the patterns and materials used bear little correspondence with natural settings (Vargas-Luna et al. 2015). Although drag on live plants was examined in the laboratory (Sand-Jensen, 2003, 2008; Statzner et al. 2006; Siniscalchi and Nikora, 2013), few studies have focused on real vegetation in natural settings, particularly at larger reach scale. For

small streams, Nikora et al. (2008) found, by comparing multiple vegetation parameters across study sites, that the best roughness descriptors while assessing the effects of SAV on hydraulic resistance were likely the ratios of average canopy/plant height to average flow depth. Their study highlights that the effect of SAV on flow could be assessed using site-averaged parameters. One such parameter is the blockage factor where flow resistance is a function of plant patches formed by multiple stems and leaves (Green, 2005). The obstruction to flow created by vegetation results in large velocity variations inside and outside of the patch (Kleeberg et al. 2010). The additional drag is represented in this case either through cross-sectional or volumetric versions of the blockage factor.

Quantifying the hydrodynamic impacts of macrophytes for large rivers or estuaries remains a challenge. The main difficulty lies in the need for an adequate representation of the added drag caused by vegetation through an apparent drag coefficient, C_D (Vargas-Luna et al. 2015). In turn, the apparent drag coefficient and flow resistance have been shown to vary markedly with physical plant features or traits such as differences in stem width and length, structural plant rigidity or flexibility, plant posture (Boothroyd et al. 2017), and the amount of foliage (Vargas-Luna et al. 2015). Differences in experimental techniques, study design and measurement methods/equipment account for the wide range of C_D reported in the literature (Statzner et al. 2006). Values of C_D for plants has been estimated as a function of 1) velocity (Sand-Jensen, 2003; O'Hare et al. 2007; Wunder et al. 2011), 2) Reynolds number (based on submerged depth of vegetation and average velocity) (Wu et al. 1999; Wilson, 2007; 2017), or 3) through other dimensions pertinent to aquatic vegetation, such as stem thickness or diameter. Stem thickness and diameter have also been used in combination with either

average flow through vegetation (Tanino and Nepf, 2008; Kothyari et al. 2009; Cheng and Nguyen, 2011) or average velocity (Wilson and Horritt, 2002; Armanini et al. 2005). There is, however, insufficient attention paid to the influence of SAV on flow at the patch scale directly within aquatic ecosystems as existent models for drag/resistance are built on small-scale physically-based empirical relationships using roughness parameters (e.g., C_D and/or Manning's n) and do not reflect the spatial variation within the flow field (Marjoribanks et al. 2017; Ayoub et al. 2018).

Another limitation in quantifying hydrodynamic impacts of SAV in numerical models at larger scales is that a numerical grid of high resolution is required to represent individual plants. Higher-resolution numerical grids increase calculation time substantially and require powerful computers or clusters to deal with multiple equations per time step. Brito et al. (2016) and Boothroyd et al. (2017) argue that for small scale study sites (4 - 20 m^2), SAV could be represented as porous media, thus eliminating the need of a high-resolution grid. However, it remains doubtful that such an approach is applicable at larger scales.

Several two-dimensional (2D) numerical models which include the impact of macrophytes for large waterbodies exist; for example, Morin et al. (2000b) and Li and Millar (2011) have represented the increased SAV in their models through elevated Manning's n values. Because most submerged plants are flexible and have different growth forms where many do not occupy the entire water column, a 3D hydrodynamic approach may better represent their true impact on the flow field. Moreover, while the effect of macrophytes on the shape of vertical velocity profiles has been previously examined in a laboratory setting (Fischer-Antze et al. 2001; Aberle and Järvelä, 2013; Hu et al. 2013; Nikora et al. 2013), to the best of our knowledge, no

previous work has attempted to use a 3D numerical model to characterise velocity profiles at a large-scale field site. The objectives of our study are to: 1) develop a 3D hydrodynamic model of a large-scale field site with abundant macrophytes (Lake Saint-Pierre, QC, Canada); and 2) compare the modelled flow field with field measurements for different vegetation configurations and patch arrangements.

6.2. Material and methods

6.2.1 Study area

Lake Saint-Pierre (LSP), a freshwater widening of the St. Lawrence River (SLR) in Quebec, Canada (Figure 6.1), is a critical area for wildlife and aquatic species (Hudon and Carignan, 2008) with significant macrophyte coverage during the summer (Vis et al. 2007). The surface of LSP covers about 300 km^2 and stretches for nearly 30 km in length (streamwise direction). The lake was chosen as a Ramsar site in 1998 (https://rsis.ramsar.org/ris/949), and in 2000 it was designated as UNESCO Biosphere Reserve (Canadian Commission for UNESCO, 2017). Several agricultural watersheds drain into LSP, mainly from the south shore (e.g., Yamaska, Saint-François, and Richelieu Rivers) (Goyette et al. 2016) and since it is located downstream from the greater Montreal area, it is also affected by urban waste water pollution (Blaise et al. 2008; Marcogliese et al. 2015). Most of the lake is relatively shallow, with an average depth of 3-4 m (Figure 6.1). A significant portion of the discharge is concentrated in the man-made central navigation channel, with depths exceeding 11 m (Hudon and Carignan, 2008). During July-August, approximately 85% of the LSP bed area is covered by submerged aquatic plants (Vis et al. 2007; Hudon and Carignan, 2008).

Starting in 2012 the strategic research cluster GRIL (Interuniversity Research Group in Limnology) initiated a macrophyte and ecosystem service monitoring program of an ~42 km^2 area of LSP downstream from the mouth of the Saint-François River (SFR) (Figure 6.1). The established zone was selected due to characteristic extensive plant colonization with high spatial variability in abundance (Vis et al. 2008, Hudon et al. 2012, de la Chenelière et al. 2014). The study zone includes approximately 60 measurement stations (Figure 6.1) that were surveyed at maximum macrophyte abundance (end of July, beginning of August) for a 6-year period (2012 to 2017).

Currently, a 2D hydrodynamic model of the St. Lawrence River is used by Environment and Climate Change Canada (ECCC), which includes LSP (Morin et al. 2000b; Martin et al. 2016). This model characterizes flow resistance due to SAV through a friction coefficient (Manning's *n*) (Boudreau et al. 1994; Talbot, 2006). Although this approach models reduced velocities in macrophyte zones, it does not represent near-zero velocity zones well, which are observed in some parts of LSP.

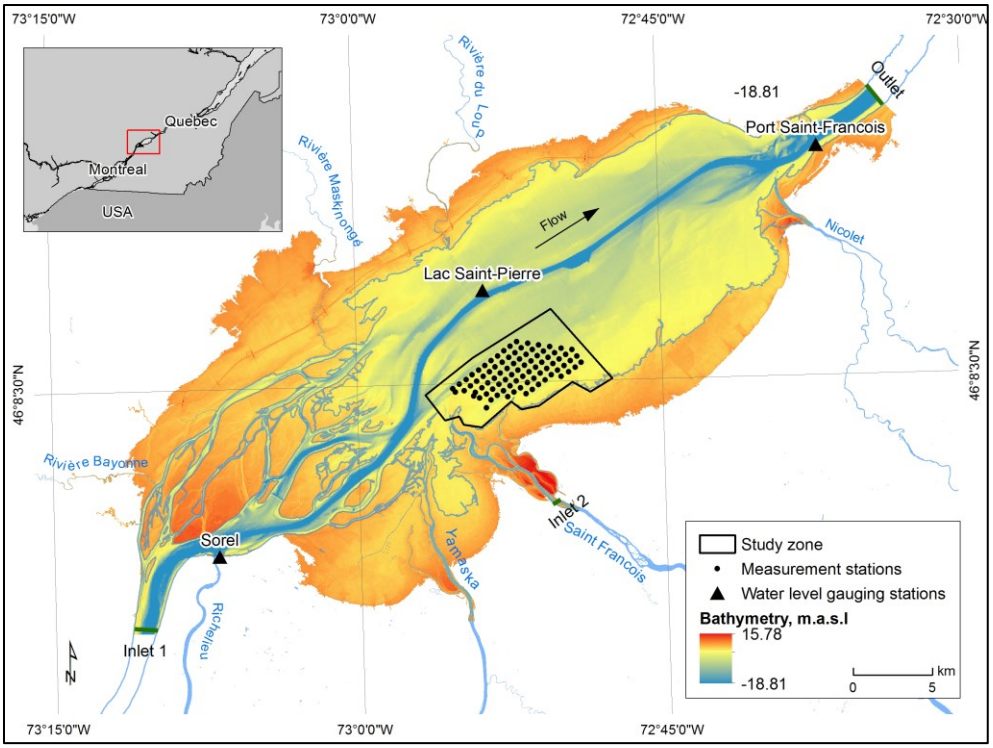

Figure 6.1. Location and bathymetry of Lake Saint-Pierre (LSP) including the study zone at the mouth of the Saint-François River. LSP is located approximately 100 km north-east of Montreal (Quebec).

6.2.2 Field data

Field measurements included the spatial distribution of macrophyte height and biomass as well as velocity measurements. Macrophyte measurements were performed annually using echosounding techniques, as well as, direct sampling using the rake method (Yin et al. 2000). Acoustic surveys were conducted on 250 m-spaced transects perpendicular to the lake shore using a downward-looking single beam BioSonics DTX system with a 6.6° angle and a working frequency of 430 kH (pulse length of 0.1 ms, ping rate 5 ping/sec). Data were post-processed in Visual Habitat 1 (BioSonics) and averaged for cycles of 5 pings. Macrophytes were also collected by raking the lake bed over a distance of about 1 m (0.35 m^2) at each station. Macrophyte biomass was estimated from the mean of three replicate rake samples collected around the boat and reported as dry mass (grams) per square meter. Velocity measurements were taken

with a propeller current meter (Swoffer 2100) at 3 (2012-2015) or 4 (2017) heights above the bed. In 2012-2015, points were taken at 20, 40 and 80% of flow depth, and in 2017 an additional measurement was taken at 60% of the depth above the bed.

Bed elevation data are particularly important for hydrodynamic model mesh generation. For our study, we used a digital elevation model (DEM) created in 2002 by ECCC. The DEM has a pixel resolution of 25 m and was created by combining LiDAR elevation and sonar bathymetry data. Measured historical water-level data were obtained from Fisheries and Oceans Canada (DFO) for the following gauging stations: Sorel (#15930, upstream section), Lake Saint-Pierre (#15975, mid-lake location) and Port Saint-François (#3365, downstream section) (Figure 6.1). The water level used in the model at the outlet boundary was linearly extrapolated using Sorel and Port Saint-Francois gauging stations. The estimated daily historical discharge data for the the St. Lawrence River at Sorel, near the inlet (Figure 6.1) was provided by ECCC (Jean Morin, *pers. comm*.). The discharge data for the Saint-François River was obtained from Hydro-Québec Chutes Hemming station (located 48 km upstream from the Saint-François River mouth). A correction of 1.05, computed based on the ratio of drainage areas, was applied to estimate the discharge at the inlet of the Saint-François River from the gauging station measurements (Inlet 2, Figure 6.1). The Yamaska, Richelieu, and other tributaries flowing into the lake were excluded from the model and considered insignificant (< 10%) in comparison to the discharge of the St. Lawrence River. Flow conditions varied between years, with 2012 representing the year with lowest discharge and flow stage for the St. Lawrence River, and 2017 the highest (Table 6.1).

Table 6.1. Mean daily discharge calculated for field data campaign dates for the St. Lawrence River (SLR) at Sorel and the Saint-François River (SFR) at its confluence with LSP used in runs.

Survey year	SLR discharge at Sorel (m^3/s)	SFR discharge (m^3/s)
2012	7450	40.6
2013	9015	107.5
2014	9955	94.5
2015	9898	135.2
2017	11305	71.5

6.2.3 Three-dimensional model: Delft3D

The model Delft3D (D3D), developed by Deltares, NL, was used in this study (version 4.01.01.rc.03, August 11, 2015). D3D is an open-source software, which allows creating hydrodynamic models of fluvial, lacustrine and coastal / tidal environments. It is based on the Navier-Stokes and continuity equations under the shallow water and the Boussinesq assumptions. The software can model flow dynamics in two and three dimensions and has the capacity to include sediment, nutrient and pollutant transport. For 3D computation, vertical velocities are computed from the continuity equation.

6.2.3.1 Selection of macrophyte modelling approach

The latest versions of D3D (since May 2014) include additional functionality to address the integration of drag due to the presence of bed forms (e.g. dunes) and macrophytes. Depending on the required type of modelling (2D or 3D), D3D offers application of two vegetation models: either trachytopes (from a Greek word meaning roughness), or a modified 3D k-ε turbulence mode (Delft3D-Flow manual, 2014). The modified 3D k-ε turbulence model was successfully tested by Fischer-Antze et al. (2001) for laboratory conditions. Trachytope

functionality defines resistance and bed roughness on a sub-grid scale (having several values per cell) through different resistance classes (referred to as trachytopes). In the modified 3D *k*-ε turbulence model, aquatic plants are represented as rigid cylinders. The main input parameters are the number of plants per unit area and stem width. The impact of vegetation on the flow is given through a vertical distribution of the drag force induced by stems. Both functionalities were preliminarily tested in a simple flume model (Bulat, 2018) whose geometry was similar to the experimental setup described in Murphy et al. (2007). The modelling results revealed little variation in velocities using the trachytope function. Alternately, the modified 3D *k*-ε turbulence model resulted in large velocity variations within the flow field, both vertically and horizontally. The predicted mean velocity profiles compared well with the measurements of Murphy et al. (2007). Based on these preliminary findings (not shown) it was decided to apply the modified 3D *k*-ε turbulence vegetation model to the main LSP model.

6.2.3.2 Model Preparation

An initial model of LSP was built using the RGFGRID module in D3D. To simplify the model, only the confluence of the St. Lawrence with Saint-François Rivers was taken into account. The upstream boundary of the LSP (the Sorel-Berthier Archipelago) has a complex geometry, comprising of approximately 103 islands. Given this complexity, a Cartesian rectangular grid was preferred to a curvilinear one to avoid continuity problems during model computation. In total, the grid consisted of 796 x 260 cells out of which 140 133 (68%) were active elements. The average cell size was around 70 m. In order to focus on the area at the mouth of the Saint-François River (study zone, Figure 6.1), a connected subgrid was required. The grids were

connected through domain decomposition where variables are transferred through the connecting boundaries. To determine the refinement factor of the subgrid, a grid sensitivity analysis was conducted with three grid resolutions (of 76 x 55 m, 25 x 20 m and 15 x 12 m) in the study zone (keeping a coarser fixed LSP grid size in all tests). Modelling results using the second grid refinement (factor of 3) revealed a percentage difference in maximum velocity from the finest resolution (refinement factor of 5) of less than 10%, which is considered a satisfactory threshold (Biron et al. 2007). The refinement factor of 3 was therefore used, resulting in average cell size in the study zone of approximately 25 m (Figure 6.2).

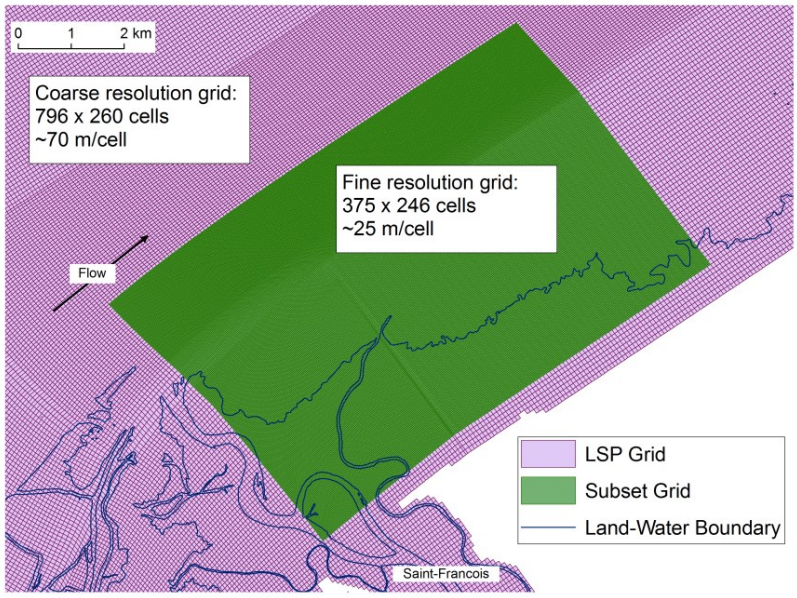

Figure 6.2. Spatial distribution of grids used in LSP model, with a finer resolution in the study zone (in green)

D3D allows utilization of different roughness coefficients including Manning's *n.* Although the simplest approach was to use a single roughness coefficient value for the entire domain, we preferred the use of a generalized roughness coefficient map, to better represent the spatial

variations in flow resistance, while considering the scale of LSP. Accordingly, the initial Manning's *n* value for the St. Lawrence (main navigational channel in the lake) and Saint-François Rivers in the model was set to 0.016, and the rest of the lake was assigned a value of 0.018 except for the study zone where *n* was equal to 0.038. These values were later modified at the calibration and validation stages.

Macrophytes in the study zone were represented via 4 scenarios:

1) Manning's *n* value,

2) Mannings's *n* and 3D *k-ε* turbulence submodel applied assuming a *homogeneous* distribution of vegetation (0.75 m in height, single stem of 0.5 cm diameter and density of 500 rigid cylinders per m^2),

3) Mannings's *n* and 3D *k-ε* turbulence submodel applied to *large patches* (based on the field observations of macrophyte coverage over 5 years (height of 0.75 m in height, 5mm diameter, 500 and 1000 cylinders/m^2 density)),

4) Mannings's *n* and 3D *k-ε* turbulence submodel applied to *small patches* 100 m x 100 m in area based on 2015 survey macrophyte data.

Sensitivity analysis on stem diameter and plant density revealed minor changes in velocity for models with thicker stems and higher plant density (Bulat, 2018). Sensitivity analyses were run for macrophyte heights and densities, starting with an average value for heights (0.35 m, based on field observations) and densities (500 cylinders/m^2, based on sensitivity analyses). These values were then progressively increased (0.65 and 1.00 m for heights, 750 and 1000

cylinders/m^2 for densities). For heights, a very high value of 1.35 m was also tested, even if in some cases this exceeded water depth, to better assess the impact of this variable on the numerical models.

6.2.4 Model Calibration and Validation

The hydrodynamic model (without vegetation) was built and calibrated using June 18, 2012 discharge and water surface data. A low flow (August 19, 2012) and high flow (October 2, 2010) condition were used for model validation by comparing modelled and measured water levels at the three gauging stations. Table 6.2 summarizes the boundary conditions used for calibration and validation. All models were run for 18 hours at steady-flow conditions and a 0.1-minute time step.

Table 6.2. Boundary conditions used for calibration and validation.

	2012/06/18	**2012/08/19**	**2010/10/02**
Q_{SLR} (m^3/s)	7990	7198	12400
Q_{SF} (m^3/s)	51	33	1151
Water $level_{SLR}$ (m)	3.37	3.23	4.88

Table 6.3. Validation results based on comparing water level at the gauging station locations.

Date	**Gauging Station**	**Measured, m**	**Modelled, m**	**Difference, m**
2012/08/19 (low flow)	Sorel	3.775	3.775	0
	Lake Saint-Pierre	3.427	3.444	0.02
	Port Saint-François	3.251	3.25	0.01
2010/10/02 (high flow)	Sorel	5.482	5.539	0.06
	Lake Saint-Pierre	5.127	5.163	0.04
	Port Saint-François	4.950	4.928	0.02

The calibration was performed by uniformly adjusting Manning's *n* values by small increments throughout the entire domain. The final values used in LSP model were *n* = 0.0235 for the main channel of the St. Lawrence River and the Saint-François River, *n* = 0.0455 for the study zone and *n* = 0.0255 for the rest of the lake. Validation results for low flow (August 19, 2012) revealed an average difference in elevation of 1 cm, whereas for the higher flow conditions (October 10, 2010), the average difference was 4 cm for the three water level stations (Table 6.3). The model thus appeared to adequately reproduce water levels of LSP under a wide range of flow conditions.

6.3. Results

6.3.1 Macrophyte distribution and parameterization

The macrophyte field data reveal high inter-annual variability in both the biomass and plant height, with higher values in 2013 and 2015 (Figure 6.3A, B). Consistent patterns of dense (30-150 g dry mass/m^2) and high (0.35 – 1.00 m) SAV were observed close to the confluence with the Saint-François River and along the right downstream bank of LSP, where macrophytes occupied up to 70% of the total water column (i.e. flow depth).

Based on an average pattern of biomass for the 5-year study period (Figure 6.3A), the large patches used in modelling scenario 3 were defined manually in a Geographical Information System (GIS) with dense (1000 plants/m^2) patches close to the right bank fringed by two smaller, more scattered (500 plants/m^2) vegetation patches located farther from the bank (large patches scenario) (Figure 6.4).

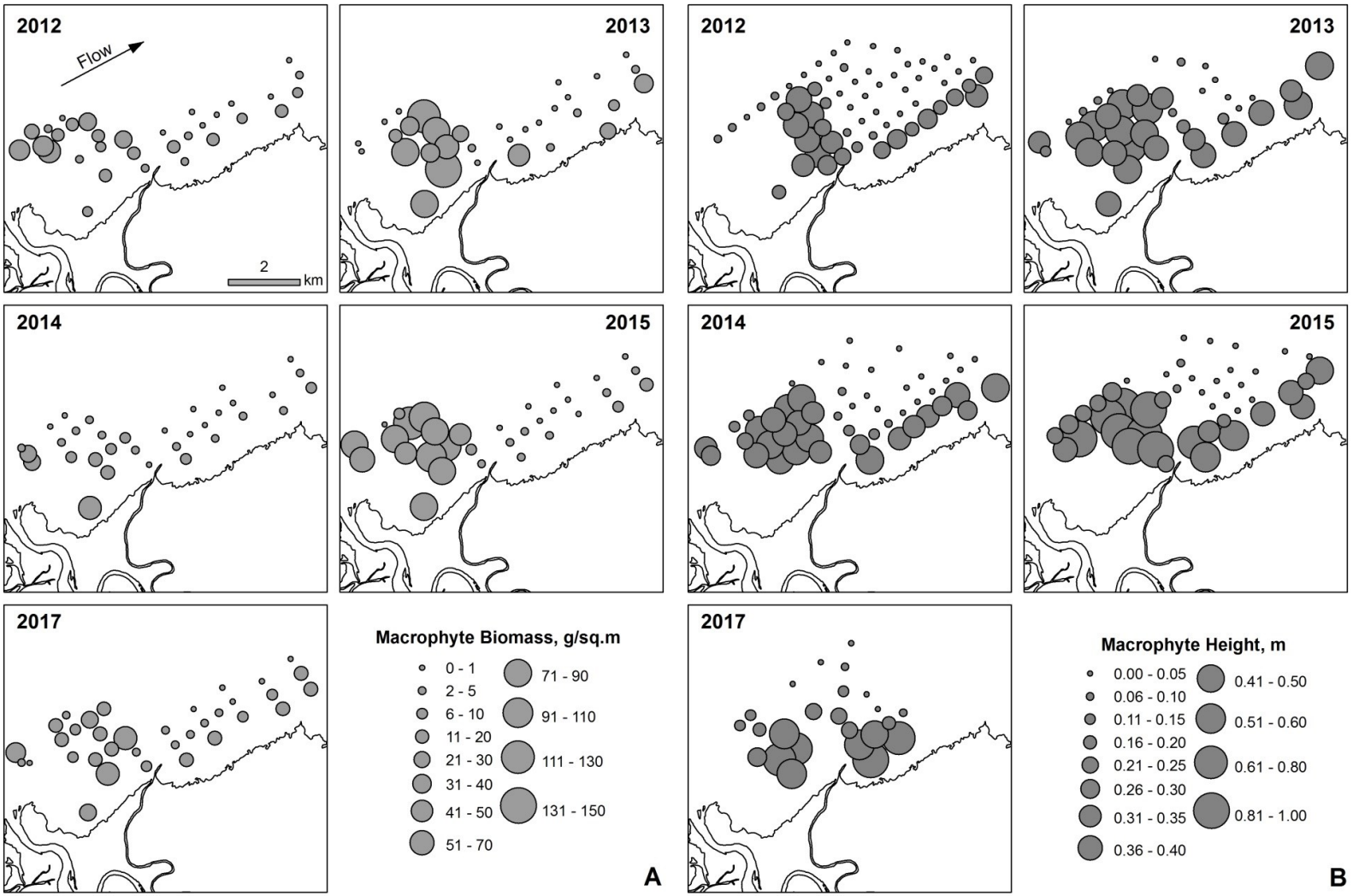

Figure 6.3. Spatial variation of total macrophyte biomass (g dry mass /m^2) collected (A) and macrophyte height (m) (B) at the measurement stations. Flow in LSP is from left to right (see arrow in upper left panel).

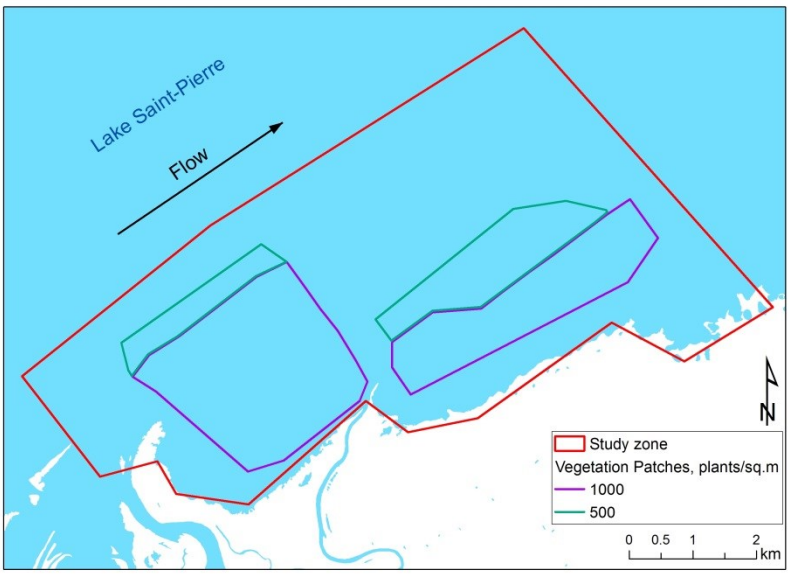

Figure 6.4. Location of the modelled patches inside the study zone with either 500 or 1000 plants/m^2 (large patches scenario).

6.3.2 Spatial distribution of velocities

Measured velocity profiles in the study zone reached a maximum of *V* = 0.34-0.50 m/s near the water surface (80% depth from the bed). Depth-averaged velocities (DAV), calculated by taking the average values at 20% and 80% of the water depth, are presented in Figure 6.5 and ranged between DAV = 0.06 and 0.11 m/s. Overall faster flow was observed farther from the bank towards the navigational channel. The flow slowed in the mid-section of the zone and reached near-zero velocities near the shore. Comparisons between the plant biomass (Figure 6.3A) and depth average velocities (Figure 6.5) show that the elevated biomass at the mouth of the Saint-François River coincided with markedly reduced velocities in the study zone (Figure 6.5).

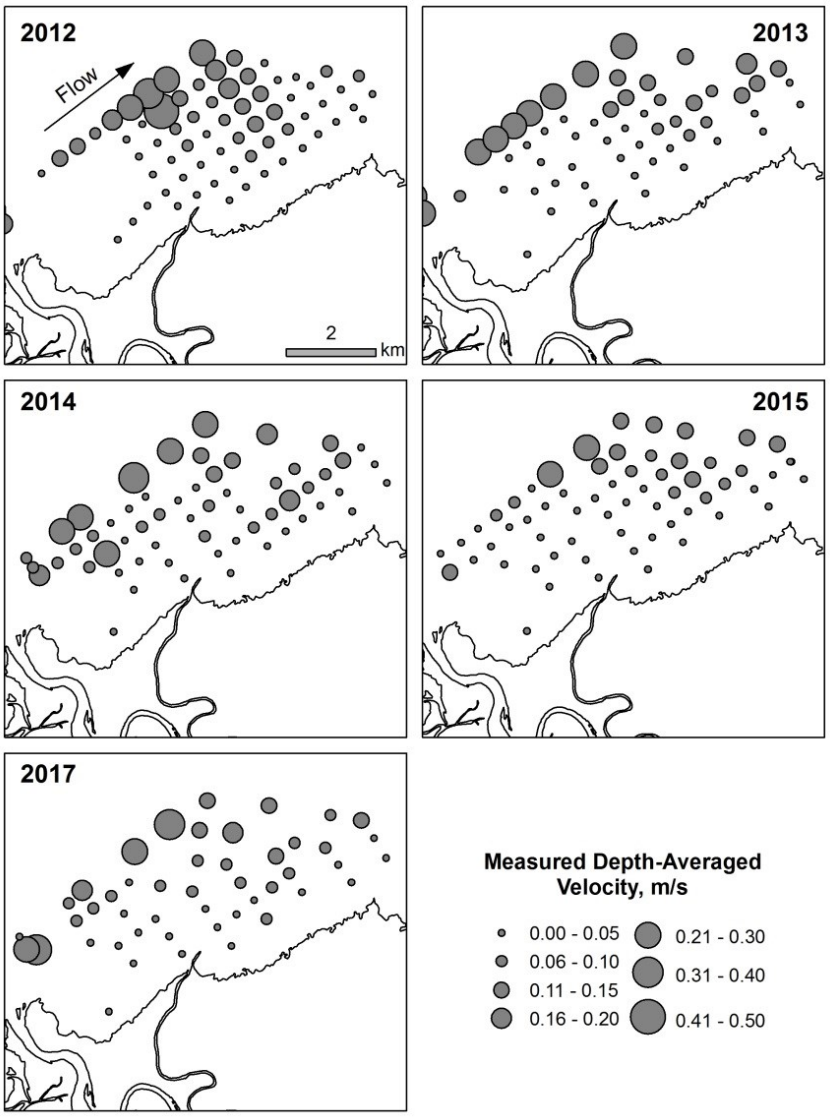

Figure 6.5. Field measurements of depth-averaged velocity (m/s) at measurement stations.

6.3.3 Numerical modelling – impacts of macrophytes on residence time

6.3.3.1 Depth-averaged results

The spatial variability in modeled water velocity is best illustrated using the depth-averaged results. The August 2017 flow condition (Q = 11,377 m^3/s) is presented in Figure 6.6A

and is representative of all the surveyed years. In Figure 6.6A, marked differences in velocity are observed between the main (navigation) channel of the St. Lawrence River, peaking at 1.2 m/s, and the markedly slower flow along the banks, including the study zone, with velocity below 0.1 m/s. The model results presented in Figure 6.6A and 6.6B are based on using Manning's *n* to represent increased macrophyte roughness near the STF confluence. Overall, the modelled flow field corresponded well to field measurements (Figure 6.6B), but there are a few stations closer to the navigational channel where the velocity is underestimated (in white in Figure 6.6B) and, most importantly, the velocity of 42.6 % of the stations, primarily near the bank, were overestimated by the model (black circles in Figure 6.6B). This highlights the limitations of a model solely based on Manning's *n* to predict very low velocities associated with macrophytes as the assumption of a logarithmic profile is unrealistic in canopies. Therefore, even with very high Manning's *n* values, the near-zero velocities would not be adequately simulated. Introducing additional drag due to macrophytes into the LSP model through the modified 3D *k-ε* turbulence submodel yielded a decrease in flow velocity with a better agreement (4.3% of the stations with overestimated velocity) with the field measurements near the right bank (Figure 6.6C).

The decrease in flow velocity resulting from the additional drag due to macrophytes through the modified 3D *k-ε* turbulence model corresponds to an increase in water retention time in the study zone. This was tested for 5 different flow events from 2012 to 2017 by comparing the first scenario (Manning's *n* only) with the models incorporating Manning's *n* and additionally the modified 3D *k-ε* turbulence model to represent macrophytes either as a

homogeneous zone covering all sampling stations (0.75-m plant height and 500 plants/m^2 density) or as large patches (Figure 6.4).

The DAV for each scenario, averaged for different flow events over the 5-year period reveal that the homogeneous distribution of macrophytes, resulted in the largest increase of mean residence time in comparison to predictions modelled using Manning's *n*. The mean residence time was estimated by dividing the longitudinal distance of the study zone, 9.7 km, by the DAV. The homogeneous distribution is seen to increase the mean residence time by 6.2 hr (Table 6.4). The inclusion of vegetation patches in the model (covering 15 km^2) is seen to exert a lesser impact on mean residence times than a homogeneous plant cover, which assumes SAV over the entire zone of 42 km^2. The patches nevertheless increased mean residence time by 3.2 hours.

Table 6.4. Comparison of mean 2012-2017 water residence time based on the spatial mean depth-averaged velocity (DAV), for the three scenarios of macrophyte roughness modeled using the 3D *k-ε* turbulence submodel.

Scenario	**Mean DAV, m/s**	**Mean DAV standard deviation, m/s**	**Mean residence time, hr**	**Mean difference in residence time, hr**
Manning's *n* only	0.120	0.0089	22.4	--
Small patches (*k-ε* submodel)	0.120	0.0700	22.4	--
Large patches (*k-ε* submodel)	0.105	0.0050	25.6	3.2
Homogeneous (*k-ε* submodel)	0.094	0.0089	28.6	6.2

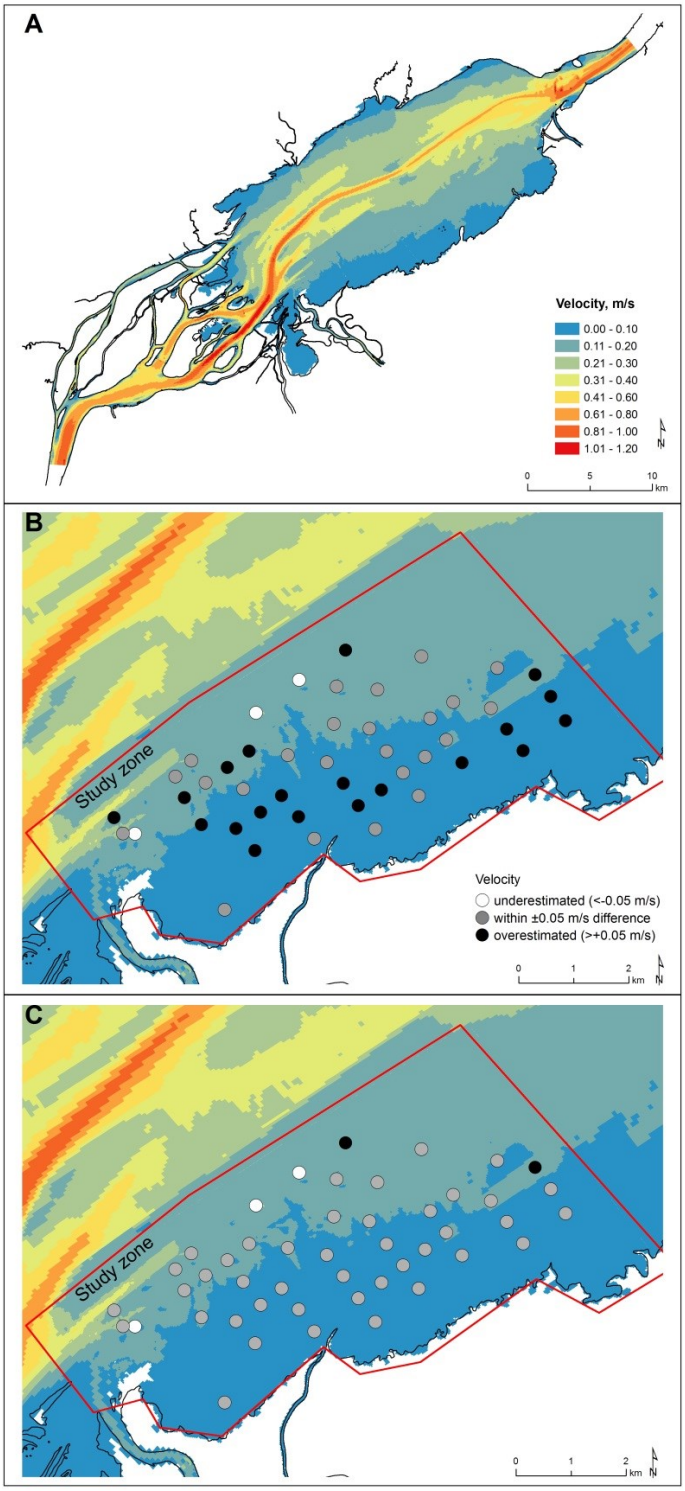

Figure 6.6. Modelled depth-averaged velocity for the August 2017 dataset: A) whole domain using Manning's *n* only; B) study zone using Manning's *n* only; and C) study zone using Manning's *n* and the 3D *k-ε* turbulence model. Velocity comparison between the predicted and measured velocity at measurement stations, showing where the model underestimates (white circles), overestimates (black circles), or approximates field observations (grey circles, within +/- 0.05 m/s).

6.3.3.2 Vertical differences in the water column

In 2015 a high density of macrophytes was measured at the field site. This year was therefore used to compare velocities and mean residence time predicted by the Manning's *n* and homogeneous models at three different relative heights above the river bed (bottom (*z/H* = 0-0.2); middle (*z/H* = 0.4-0.6); surface layer (*z/H* = 0.8-1.0), where *z* is the height above the bed and *H* was the total depth at a specific location. Statistical analysis (t-test, $\alpha = 0.05$) showed that the mean velocity modelled using the homogeneous macrophyte distribution and *k-ε* model were significantly reduced near the river bed and in the middle of the water column in comparison with Manning's n only model (Figure 6.7, Table 6.5). Accordingly, mean residence times for the homogeneous scenario were increased by 5.8 hr in the middle layer and 22.8 hr in the bottom layer, assuming a parcel of fluid remains at the same elevation as it advects downstream. No significant difference in top-layer (near surface) mean velocity or residence time between values predicted using the Manning's *n* only model and that derived from the homogeneous macrophyte distribution with *k-ε* model.

Table 6.5. Comparison of mean longitudinal velocity and mean water residence time between the Manning's n only and homogeneous SAV with *k-ε* modelling methods for 3 vertical water layers located at increasing height above the river bed.

Layer *z/H*	**Mean velocity, m/s**		**Standard deviation, m/s**		**Residence Time, hr**		**Difference, hr**
	Manning's n only	*Homogeneous, k-ε submodel*	*Manning's n only*	*Homogeneous, k-ε submodel*	*Manning's n only*	*Homogeneous, k-ε submodel*	
Top (0.8-1.0)	0.15	0.14	0.08	0.01	17.9	19.2	1.3
Middle (0.4-0.6)	0.13	0.10	0.07	0.09	21.0	26.8	5.8
Bottom (0-0.2)	0.078	0.047	0.05	0.06	34.6	57.4	22.8

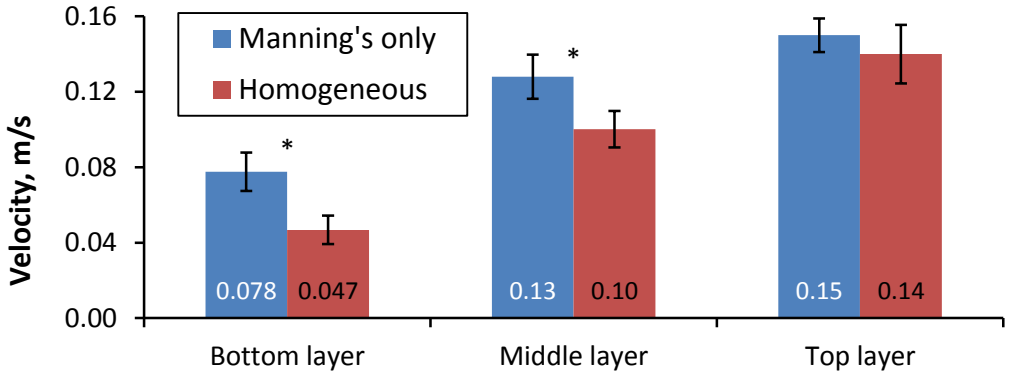

Figure 6.7. Comparison of mean velocity for the whole study zone derived from values modelled using Manning's *n* or homogeneous macrophyte distribution scenarios (with *k-ε* submodel). Velocity values were modelled separately for the bottom layer near the river bed (*z/H* = 0-0.2), in the middle layer (*z/H* = 0.4-0.6), and in the surface (top) layer (*z/H* = 0.8-1.0) of the water column. Significant differences in velocity are indicated by the star symbol.

6.3.4 Numerical modelling – comparison with field observations

6.3.4.1 Correlation analyses

As presented in Section 3.1, we tested the effect of smaller vegetation patches of 100 x 100 m centered on each measurement station with reported macrophytes during the 2015 survey, leaving the rest of the zone free of SAV. The impact of these small patches on the overall DAV was small with the mean velocity remaining at 0.12 m/s, regardless of the parameter values used for plant densities (500, 750 or 1000 plants/m^2) and plant heights (0.35, 0.65 and 1.00 m). This was not surprising since the relative area allocated to macrophytes remained very small, occupying only 0.76 % of the study zone.

The direct comparison between measured and modelled velocity data (station by station) is presented in Figure 6.8. The regression slope can be seen to approach unity with the *k-ε* model. This is likely due to the model's ability to better predict the low velocities found in the macrophyte zones. Local comparisons of velocity using only Manning's *n* showed relatively low

correlations r = 0.461. When using the *k-ε* submodel the correlation increased, particularly for higher plant heights (Table 6.6). The modelled macrophyte height thus appears as the main driver in the increase of agreement between the measured and predicted velocities, while densification of macrophyte patches caused only minor changes. This supports the conclusion of Vargas-Luna et al. (2015) that the degree of submergence was the major factor driving flow resistance estimation. The largest correlation value (0.804 for DAV) was associated with plants (rigid cylinders) of 1.35 m. It is worth noting that at some sampling stations this height exceeded the total water depth, therefore resulting in a shift from fully submerged to surface floating.

Table 6.6. Pearson correlation (*r*) values for the comparison of modeled and measured velocities at different heights above the bottom as well as depth-averaged (DAV). All comparisons are based on 62 observations for the year 2015.

Model scenarios		**Correlation with measured velocities in each water layer / Depth averaged velocity**			
Plant height, m	**Plant density, plants/m^2**	**Bottom 0-20%**	**Middle 20-40%**	**Top 80-100%**	**DAV**
0.35	750	0.677	0.693	0.490	0.682
0.65	500	0.690	0.771	0.633	0.744
0.65	750	0.689	0.769	0.616	0.741
0.65	1000	0.689	0.769	0.602	0.738
1.00	750	0.695	0.785	0.742	0.790
1.00	1000	0.695	0.784	0.739	0.789
1.35	1000	0.699	0.789	0.783	0.804

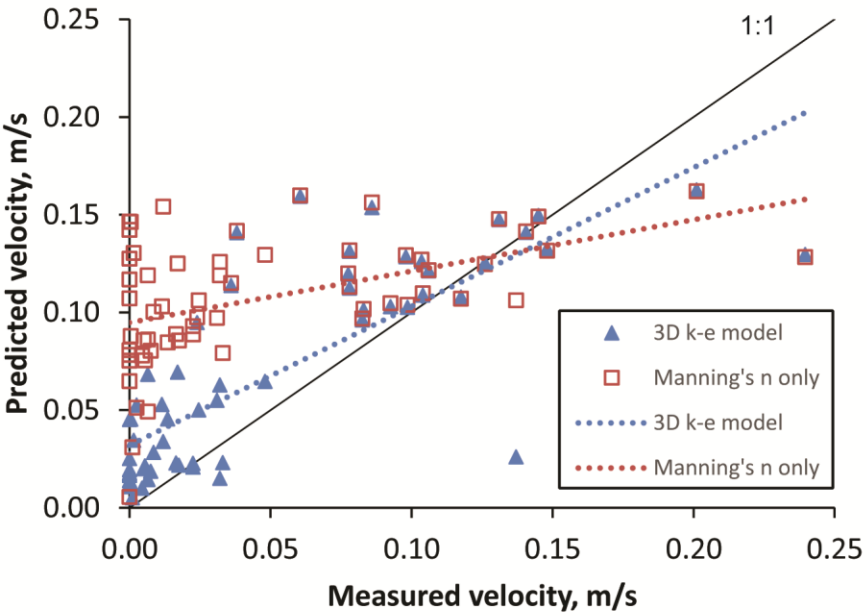

Figure 6.8. Predicted versus measured velocity for the 2015 models using Manning's *n* only (red squares) and k-ε model for depth-averaged velocity (blue triangles).

6.3.3.2 Comparison of vertical velocity profiles at specific stations

Velocity profiles modelled using the small-patch vegetation method (*k-ε* submodel) and the 2015 data were used to compared with velocities generated from the Manning's *n* only model and with field measurements. Figure 6.9A-D presents cases with a very good match between field velocity measurements and predicted velocities when using the modified 3D *k-ε* turbulence model at four measurement stations. In these cases, the Manning's *n* only models (logarithmic profile) are clearly overestimating velocity. It is interesting to note that the modified *k-ε* turbulence model is able to well predict both the cases with near-zero velocity (Figure 6.9A, B) and with a slow, but non-zero velocity (Figure 6.9C, D). There are, however, also cases where neither the Manning's *n* nor the modified *k-ε* turbulence model has been able to model field observations (Figure 6.9E, F). For the cases where no macrophytes are reported

(Figure 6.9G, H), the Manning's *n* only scenario results in a fairly good agreement with the measured vertical profile.

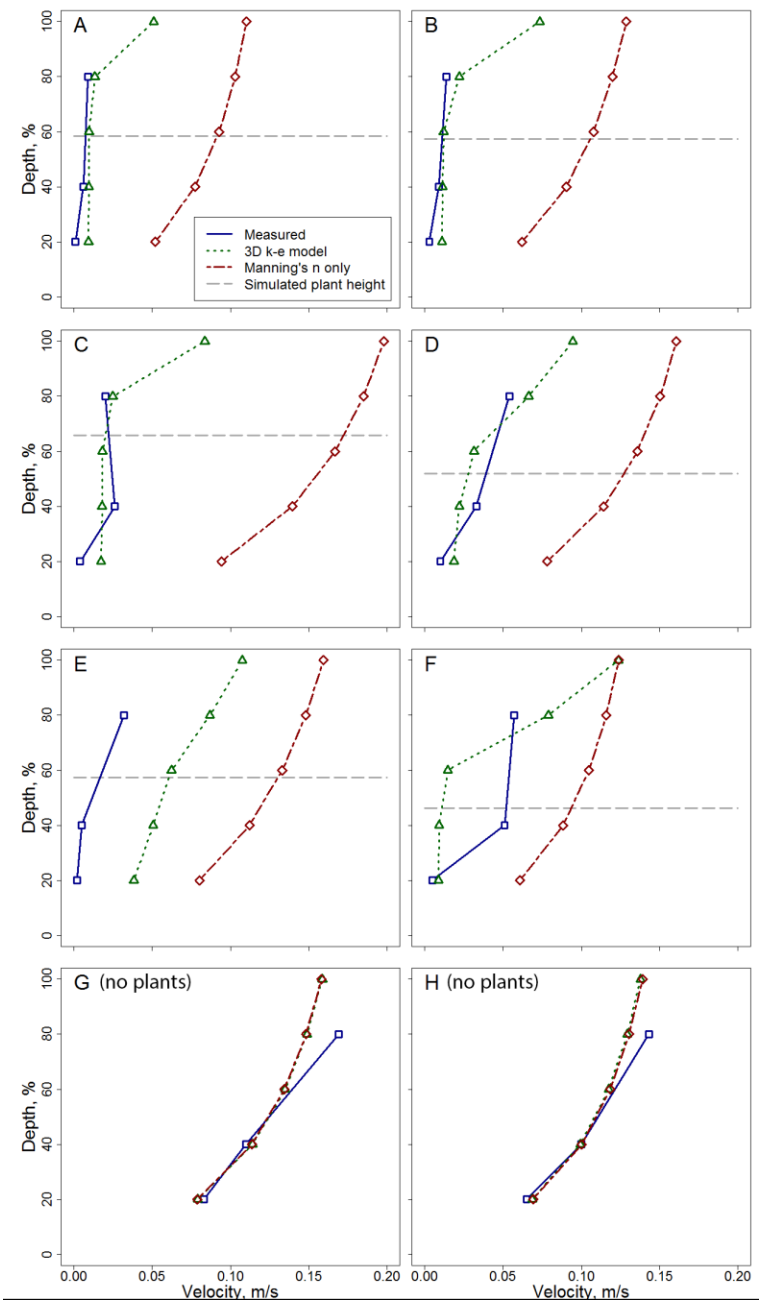

Figure 6.9. Comparison of modelled and measured velocity profiles at different measurement stations in 2015: A to H macrophytes present; and G and H – no reported macrophytes. Based on field measurements, macrophytes were characterized having 1-m height and 750 plants/m^2 density in A-C, E and F; 0.65 m height and 500 plants/m^2 density in D.

6.4. Discussion

This study demonstrates the successful use of a 3D hydrodynamic model to accurately assess the impact of SAV on the flow field and mean residence time in the realistic setting of a large fluvial lake. The results from this study were validated using a unique and extensive field dataset in Lake Saint-Pierre of both macrophyte density and height, as well as velocity measurements for 5 different years. The data set has allowed for the comparison of different modelling approaches that were subsequently validated with field data.

In order to adequately represent macrophytes in the LSP fluvial system, which if very large (47 km by 13 km including the archipelago) and in particular the study zone (approximately 42 km^2), macrophytes were represented as patches instead of individual plants - a scale that currently suffers from a paucity of studies (Nepf, 2012b, Marjoribanks et al. 2017). Our results are consistent with findings from previous studies, which observed a marked effect of macrophytes on the flow field (Boudreau et al. 1994; Morin et al. 2000b; Fischer-Antze et al. 2001; Morin et al. 2003; Marjoribanks et al. 2014; 2017), and showed how the introduction of the 3D k-ε turbulence model improved the accuracy of the model. It is encouraging that the relatively simple approach used in the D3D model of LSP, based on rigid cylinders, resulted in a significant flow reduction at the depths occupied by modelled macrophytes in comparison to runs where macrophytes were represented through Manning's n only. Velocity profiles and residence time near the river bed predicted from the modified 3D k-ε turbulence model indicated an increase in drag resulting from the presence of macrophytes. While many previous studies similarly compared velocity profiles at point locations, this was done primarily in

laboratory flumes or smaller reaches (Murphy et al. 2007). The D3D LSP model successfully predicted velocities at point locations throughout the very large study zone (42 km^2).

At a reach scale, the additional resistance due to vegetation can be determined conventionally by the blockage factor (Greene, 2005; Nikora et al. 2008; Nepf, 2012b), which corresponds to a ratio of the cross-section occupied by a vegetation patch over the total cross section. However, such an approach is challenging to implement in a larger water body such as LSP, particularly when only a portion of the lake is studied.

Knowing the predicted variation of the flow field vertically enables an accurate estimate of residence time - a critical variable for understanding and predicting phosphorous and nitrogen transformations (Saunders and Kalff 2001; Blanton et al. 2010; Hensley et al. 2015). The modelled mean residence time based on DAV did not change markedly between the different tested macrophyte scenarios, reflecting the small changes in mean velocity between the runs (Table 6.4). However, calculating mean residence time for each depth layer revealed large vertical differences in water circulation, with potential impacts on nutrient retention and absorption rates (Table 6.5). Since biogeochemical transformations largely occur at the water-sediment interface due to strong redox gradients (Jaynes and Carpenter, 1986; Barko et al. 1991; Vila-Costa et al. 2016), the presence of macrophytes is likely to increase biological retention of nutrients and contaminants through increased particle settling and the enhanced residence time of near-bottom waters. This is a main advantage of the 3D model used here, as it has the ability to predict velocities at different depths due to its use of the Navier-Stokes equations, compared to more conventionally used 2D models (based on the St. Venant

equations) for study zones as extensive as LSP. Indeed, results from our study could potentially help to better understand the ecological services provided by macrophytes with regards to various biogeochemical transformations, both horizontally as well as vertically in the water column.

Although the modified 3D *k-ε* turbulence model produces hydraulically reasonable predictions for both low and high flow stage conditions of LSP, it is rather difficult to obtain a perfect fit between measured data and predictions at certain sampling station locations (Table 6.6, Figure 6.9G and H). The errors in predicting velocity could be attributed to several reasons, including the numerical mesh for the study zone, which remains fairly coarse (25 m). Marjoribanks et al. (2017) noted an improved agreement between predicted results and measured data as they increased their model mesh resolution. In our mesh resolution sensitivity tests, we concluded that the additional refinement of the study zone subdomain did not produce considerable changes in the mean velocity. Realistically, considering the scale of LSP, increasing the model mesh resolution further would have resulted in lengthy computational times or model stability issues, greatly limiting our ability to run sensitivity analysis on various macrophyte parameters. Given the scale of the study zone, the LSP model calculates a velocity value (per vertical layer) for a cell with an area of 625 m^2; thus it is not surprising that the predicted velocity differs from the observed measurements at some measuring stations located in more dynamic zones. Furthermore, the geolocation of the field data measurements does not necessarily coincide spatially with the location of the centre of a cell value in the D3D mesh.

Another explanation for the poor predictions at some sites is that the DEM used to generate the numerical mesh has a pixel resolution of 25 m, which represents a coarse generalization of the actual lake bed. Considering that the DEM was produced in 2002, it is likely that changes in the actual lake bathymetry have occurred due to aggradation or erosion, which has not been accounted for in the model. The confluence of Saint-François and St. Lawrence Rivers could be characterized as a deltaic depositional environment and there is a probability that the presence of SAV enhances further deposition. Acquiring an updated bathymetry would be valuable for future studies.

Our modelled macrophyte representation is somewhat simplified in comparison to real life conditions where there is large variability in macrophyte height and stem width both within and among different species of plants. Considering that the submerged plants are parametrized as rigid cylinders by the modified 3D k-ε turbulence model, the modelled plants are still far from the correct depiction of the in situ aquatic plants. Since in nature most of macrophytes are flexible and bend in the direction of the flow, the height used in the model actually represents bending height, which changes with water depth and velocity. Furthermore, in our models, vegetation patches were represented as blocks static in time, which would not react to changes in hydraulic parameters. Incorporating the ability to represent plant reconfiguration in modelling would benefit further studies on macrophyte-flow interactions by assessing the impact of flexible submerged aquatic vegetation, and thus better approximate the natural conditions in modelling (Marjoribanks et al. 2016; Verschoren et al. 2016).

In spite of these drawbacks, the modelling of macrophytes in our large-scale application still produced realistic resistance to flow, where the model was able to capture near-zero velocities as measured in situ. This is a major contribution as obtaining reliable velocity measurements in large water bodies affected by macrophytes is notoriously difficult (Ayoub et al. 2018). Considering that the D3D model is capable of approximating measured velocity magnitude, preserving the logarithmic shape throughout the water column and reaching near-zero velocities without increasing the roughness coefficient, we recommend this modelling approach for future research on the impact of macrophytes on flow at the scale of vegetation patches in large water bodies comparable to Lake Saint-Pierre.

Conclusions

A 3D hydrodynamic model that represents macrophytes through a modified 3D *k-ε* turbulence model in Delft3D was successfully used to model the observed flow field in Lake Saint-Pierre, a large fluvial lake in the St. Lawrence River system. When compared to the more traditional modelling approach using a resistance coefficient (Manning's *n*), predicted velocities were in better agreement with field data. Modelled residence time in an extensive zone with an area of 42 km^2 downstream from the confluence with the Saint-François River was also longer than that predicted from the Manning's *n* approach, particularly close to the bed. Sensitivity analysis revealed that the additional resistance time is closely associated with plant height, and that plant density only plays a minor role. These findings indicate that it is possible to accurately quantify the impact of submerged aquatic vegetation on the flow field in large fluvial

systems. Such a 3D modelling approach could be used in future studies to improve our understanding on the role of macrophytes in nutrient and pollutant dynamics for a wide range of scales.

Acknowledgements

We are grateful to Stéphanie Massé, Caroline Chartier, Elena Neszvecsko, Geneviève Trottier, Magali Noiseux-Laurin, François Messier, William Massey, Joanna Gauthier, Yasmina Remnal, Jean-Pierre Amyot, Conrad Beauvais, Maude Lachapelle and Roger Gladu for their assistance in collecting field data.

This research was funded by the Fonds de recherche de Quebec – Nature et Technologies (FRQNT) scholarships (M. Bulat, M. Botrel), FRQNT Strategic Initiatives for Innovation, and Natural Sciences and Engineering Research Council of Canada (NSERC) (Discovery grants P. Biron, J. Lacey, R. Maranger), Fonds de recherche du Quebec (C. Hudon). This study is a contribution to the Canada-Québec St. Lawrence Action Plan.

The authors declare no conflict of interest.

7. General conclusions

Through the application of a 3D hydrodynamic model of Lake Saint-Pierre (LSP) and combination of novel quantitative approaches in impact assessment of submerged vegetation on flow dynamics, this study has demonstrated the potential of modelling the additional drag due to macrophytes in large-scale open-channel waterbodies. Such models allow for the accurate estimations of velocity and water residence time, which are variables highly relevant for phosphorus retention and nitrogen transformation studies. Among the many available approaches of macrophyte incorporation into hydrodynamics models, three approaches were tested in a small flume model using Delft3D, namely an increase of Manning's n value only, the 2D trachytope #154 function, and a modified 3D k-ε turbulence closure model. Findings indicate that the conventionally used Manning's n coefficient is not the best representation of the increased drag due to macrophytes in comparison to the other tested approaches. The trachytope function, which in theory should be able to take into account drag due to vegetation, did not perform well in the flume tests. Therefore, despite higher computational requirements compared to a 2D model, the modified 3D k-ε turbulence model is the most suitable approach for modelling three-dimensionally macrophytes on a larger scale. Sensitivity analyses on cylinder height and stem density indicate that the height of cylinders is a better predictor of decreased velocities in macrophyte zone than the stem densities, which had minimal effect on the modelled velocities.

There was a very good agreement between the modelled velocities in LSP and the field measurements collected through a GRIL project, which is very encouraging for future use of this

modelling approach in other large water bodies. However, future work should consider improving the model mesh to better represent complex bathymetry such as that present in the Berthier-Sorel archipelago. The future releases of Delft3D with a flexible mesh component should produce better results than the Cartesian grid used in this study. This would also allow including smaller tributaries and offering grid refinement options that would not require resorting to domain decomposition. A better representation of Manning's *n* roughness coefficient spatial variability in the lake would potentially reduce some discrepancies found between the predicted and measured velocities in some areas of the study zone, and would contribute to even better agreement between velocity predictions and observations. Since the most advanced approach available so far in Delft3D simulates plants as rigid cylinders, macrophytes might be represented too generally. Stem and leaf flexibility and reconfiguration due to flow pressure currently remain to be incorporated into Delft3D. Last but not least, the original bathymetry used for Delft3D depth files generation originates from 2002, which could possibly result in biased velocity predictions.

It is clear however that by applying the modified 3D *k*-*ε* turbulence model, the integration of additional drag due to submerged aquatic vegetation significantly lowers velocities near the bed and in mid water column, thus affecting water residence time. This may have implications for further studies that focus on nutrient budgets in the zone and could potentially provide answers to some questions raised by other researchers.

References:

Aberle, J., & Järvelä, J. (2013). Flow resistance of emergent rigid and flexible floodplain vegetation. *Journal of Hydraulic Research*, *51*(1), 33-45.

Armanini, A., Righetti, M., & Grisenti, P. (2005). Direct measurement of vegetation resistance in prototype scale. *Journal of Hydraulic Research*, *43*(5), 481-487.

Ayoub, F., Jones, C. E., Lamb, M. P., Holt, B., Shaw, J. B., Mohrig, D., & Wagner, W. (2018). Inferring surface currents within submerged, vegetated deltaic islands and wetlands from multi-pass airborne SAR. *Remote Sensing of Environment*, 212, 148-160.

Bal, K. D., Brion, N., Woulé-Ebongué, V., Schoelynck, J., Jooste, A., Barrón, C., ... & Bouma, T. J. (2013). Influence of hydraulics on the uptake of ammonium by two freshwater plants. *Freshwater Biology*, 58(12), 2452-2463.

Barko, J. W., Gunnison, D., & Carpenter, S. R. (1991). Sediment interactions with submersed macrophyte growth and community dynamics. *Aquatic Botany*, *41*(1-3), 41-65.

Baptist, M. J. (2005). *Modelling floodplain biogeomorphology*. TU Delft, Delft University of Technology.

Billen, G., Garnier, J., Ficht, A., & Cun, C. (2001). Modeling the response of water quality in the Seine River estuary to human activity in its watershed over the last 50 years. *Estuaries and Coasts*, 24(6), 977-993.

Biron, P. M., Haltigin, T. W., Hardy, R. J., & Lapointe, M. F. (2007). Assessing different methods of generating a three-dimensional numerical model mesh for a complex stream bed topography. *International Journal of Computational Fluid Dynamics*, *21*(1), 37-47.

Blaise, C., Gagné, F., Eullaffroy, P., & Férard, J. F. (2008). Ecotoxicity of selected pharmaceuticals of urban origin discharged to the Saint-Lawrence river (Québec, Canada): a review. *Brazilian Journal of Aquatic Science and Technology*, *10*(2), 29-51.

Blanton, J. O., Garrett, A. J., Bollinger, J. S., Hayes, D. W., Koffman, L. D., Amft, J., & Moore, T. (2010). Transport and retention of a conservative tracer in an isolated creek–marsh system. *Estuarine, Coastal and Shelf Science*, 87(2), 333-345.

Bolduc, P., Bertolo, A., & Pinel-Alloul, B. (2016). Does submerged aquatic vegetation shape zooplankton community structure and functional diversity? A test with a shallow fluvial lake system. *Hydrobiologia*, *778*(1), 151-165.

Boothroyd, R. J., Hardy, R. J., Warburton, J., & Marjoribanks, T. I. (2015). The importance of accurately representing submerged vegetation morphology in the numerical prediction of complex river flow. *Earth Surface Processes and Landforms*.

Boothroyd, R. J., Hardy, R. J., Warburton, J., & Marjoribanks, T. I. (2017) Modeling complex flow structures and drag around a submerged plant of varied posture. *Water Resources Research*, 53, doi:10.1002/2016WR020186

Boudreau, P., Leclerc, M., & Fortin, G. R. (1994). Modélisation hydrodynamique du lac Saint-Pierre, fleuve Saint-Laurent: l'influence de la végétation aquatique. Canadian Journal of Civil Engineering, 21(3), 471-489.

Brito, M., Fernandes, J., & Leal, J. B. (2016). Porous media approach for RANS simulation of compound open-channel flows with submerged vegetated floodplains. *Environmental Fluid Mechanics*, 16(6), 1247-1266.

Boyer, C., Verhaar, P. M., Roy, A. G., Biron, P. M., & Morin, J. (2010). Impacts of environmental changes on the hydrology and sedimentary processes at the confluence of St. Lawrence tributaries: potential effects on fluvial ecosystems. Hydrobiologia, 647*(1)*, 163-183.

Brito, M., Fernandes, J., & Leal, J. B. (2016). Porous media approach for RANS simulation of compound open-channel flows with submerged vegetated floodplains. *Environmental Fluid Mechanics*, 16(6), 1247-1266.

Bulat, M. (in. prep). *Three dimensional hydrodynamics modelling of the impact of macrophytes in Lake Saint-Pierre* (Unpublished MSc thesis). Concordia University, Montreal.

Canadian Commission for UNESCO - Commission Canadienne pour l'UNESCO. (n.d.). Biosphere Reserves in Canada. Retrieved March 27, 2017, from http://unesco.ca/home-accueil/biosphere%20new/biosphere%20reserves%20in%20canada-%20reserves%20de%20la%20biosphere%20au%20canada

Carpenter, S. R., & Lodge, D. M. (1986) Effects of submersed macrophytes on ecosystem processes. *Aquatic Botany*, 26, 341-370.

Cattaneo, A., Hudon, C., Vis, C., & Gagnon, P. (2013). Hydrological control of filamentous green algae in a large fluvial lake (Lake Saint-Pierre, St. Lawrence River, Canada). Journal of Great Lakes Research, 39(3), 409-419.

Cheng, N. S. (2011). Representative roughness height of submerged vegetation. *Water Resources Research*, *47*(8).

Cheng, N. S., & Nguyen, H. T. (2011). Hydraulic radius for evaluating resistance induced by simulated emergent vegetation in open-channel flows.

Costa, M. B., Tavares, F. V., Martinez, C. B., Colares, I. G., & Martins, C. D. M. G. (2018). Accumulation and effects of copper on aquatic macrophytes Potamogeton pectinatus L.: Potential application to environmental monitoring and phytoremediation. *Ecotoxicology and environmental safety*, *155*, 117-124.

de La Chenelière, V., Brodeur, P., & Mingelbier, M. (2014). Restauration des habitats du lac Saint-Pierre: un prérequis au rétablissement de la perchaude. *Le naturaliste canadien*, *138*(2), 50-61.

Delft3D-FLOW Manual (2014). Delft3D - 3D/2D modelling suite for integral water solutions - Hydro-Morphodynamic s. Deltares, Delft. Version 3.15.34158.

Dijkstra, J. T., & Uittenbogaard, R. E. (2010). Modeling the interaction between flow and highly flexible aquatic vegetation. *Water Resources Research*, *46*(12).

Dunn, C., Lopez, F. & Garcia, M. H. (1996). Mean Flow and Turbulence in a Laboratory Channel with Simulated Vegetation (HES 51).

eMonocot Team Classification (2018). *Potamogetonaceae.* Retrieved from http://potamogetonaceae.e-monocot.org/taxonomy/term/500/media on 20.092018

Environment and Climate Change Canada (2017), SHOP H2D2 model water level and velocity predictions. Accessed and retrieved on February 02, 2017 at http://collaboration.cmc.ec.gc.ca/cmc/cmoi/SHOP/images/.

Fischer. C. (2011). Parts of the Western Waterweed (*Elodea nuttallii*). Retrieved from https://commons.wikimedia.org/wiki/File:ElodeaNuttallii2.jpg on 20.09.2018

Fischer-Antze, T., Stoesser, T., Bates, P., & Olsen, N. R. B. (2001). 3D numerical modelling of open-channel flow with submerged vegetation. *Journal of Hydraulic Research*, *39*(3), 303-310.

Fredlyfish4 (2016). *Vallisneria americana* growing in Bay Springs Branch at the University of Mississippi Field Station. Retrieved from https://commons.wikimedia.org/wiki/File:Vallisneria_americana_UMFS_3.JPG#filelinks on 20.09.2018

Fritzflohrreynolds (2012). Photo of *Heteranthera dubia* in flower. Retrieved from https://commons.wikimedia.org/wiki/File:Heteranthera_dubia_-_Grassleaf_Mudplantain.jpg on 20.09.2018

Garnier, J., Némery, J., Billen, G., & Théry, S. (2005). Nutrient dynamics and control of eutrophication in the Marne River system: modelling the role of exchangeable phosphorus. *Journal of Hydrology*, 304(1), 397-412.

Giraudo, M., Bruneau, A., Gendron, A. D., Brodeur, P., Pilote, M., Marcogliese, D. J., ... & Houde, M. (2016). Integrated spatial health assessment of yellow perch (Perca flavescens) populations from the St. Lawrence River, Quebec, Canada) part a: physiological parameters and pathogen assessment. Environmental Science and Pollution Research, 1-12.

Green, J. C. (2005a). Modelling flow resistance in vegetated streams: review and development of new theory. *Hydrological Processes: An International Journal*, *19*(6), 1245-1259.

Green, J. C. (2005b). Comparison of blockage factors in modelling the resistance of channels containing submerged macrophytes. *River research and applications*, *21*(6), 671-686.

Grenouillet, G., Pont, D., & Olivier, J. M. (2001). Linking zooplankton and juvenile fish assemblages in a large lowland river: influence of submerged macrophytes. *Archiv für Hydrobiologie*, 383-404.

Hensley, R. T., Cohen, M. J., & Korhnak, L. V. (2015). Hydraulic effects on nitrogen removal in a tidal spring-fed river. *Water Resources Research*, 51(3), 1443-1456.

Hoffmann, M. R. (2004). Application of a simple space-time averaged porous media model to flow in densely vegetated channels. *Journal of Porous Media*, *7*(3).

Hu, Y., Huai, W., & Han, J. (2013). Analytical solution for vertical profile of streamwise velocity in open-channel flow with submerged vegetation. *Environmental fluid mechanics*, *13*(4), 389-402.

Hudon, C., & Carignan, R. (2008). Cumulative impacts of hydrology and human activities on water quality in the St. Lawrence River (Lake Saint-Pierre, Quebec, Canada). Canadian Journal of Fisheries and Aquatic Sciences, 65(6), 1165-1180.

Hudon, C., Cattaneo, A., Poirier, A. M. T., Brodeur, P., Dumont, P., Mailhot, Y., ... & de Lafontaine, Y. (2012). Oligotrophication from wetland epuration alters the riverine trophic network and carrying capacity for fish. *Aquatic sciences*, *74*(3), 495-511.

Huthoff, F. (2007). Modeling hydraulic resistance of floodplain vegetation. University of Twente.

Hygelund, B., & Manga, M. (2003). Field measurements of drag coefficients for model large woody debris. *Geomorphology*, 51(1-3), 175-185.

Ishikawa, Y., Sakamoto, T., & Mizuhara, K. (2003). Effect of density of riparian vegetation on effective tractive force. *Journal of Forest Research*, *8*(4), 235-246.

James, C. S., Birkhead, A. L., Jordanova, A. A., & O'sullivan, J. J. (2004). Flow resistance of emergent vegetation. *Journal of Hydraulic Research*, *42*(4), 390-398.

Janse, J. H. (1997). A model of nutrient dynamics in shallow lakes in relation to multiple stable states. *Hydrobiologia*, 342, 1-8.

Järvelä, J. (2003, September). Influence of vegetation on flow structure in floodplains and wetlands. In *Proceedings of the 3rd Symposium on River, Coastal and Estuarine Morphodynamics (RCEM) Madrid* (pp. 845-856).

Jaynes, M. L., & Carpenter, S. R. (1986). Effects of vascular and nonvascular macrophytes on sediment redox and solute dynamics. *Ecology*, *67*(4), 875-882.

Jeppesen, E., Sondergaard, E., Sondergaard, M., & Christofferson, K. (1997) *The Structuring Role of Submerged Macrophytes in Lakes*, Springer.

Justić, D., Rabalais, N. N., & Turner, R. E. (2002). Modeling the impacts of decadal changes in riverine nutrient fluxes on coastal eutrophication near the Mississippi River Delta. *Ecological Modelling*, 152(1), 33-46.

Katayama, M. (2014). Stem stiffness plays a role in determining the foraging success of predators. *Hydrobiologia*, 732(1), 173-181.

Kleeberg, A., Köhler, J. A. N., Sukhodolova, T., & Sukhodolov, A. (2010). Effects of aquatic macrophytes on organic matter deposition, resuspension and phosphorus entrainment in a lowland river. *Freshwater Biology*, 55(2), 326-345.

Kothyari, U. C., Hashimoto, H., & Hayashi, K. (2009). Effect of tall vegetation on sediment transport by channel flows. *Journal of Hydraulic Research*, *47*(6), 700-710.

King, A. T., Tinoco, R. O., & Cowen, E. A. (2012). A k–ε turbulence model based on the scales of vertical shear and stem wakes valid for emergent and submerged vegetated flows. *Journal of Fluid Mechanics*, *701*, 1-39.

Klopstra, D., Barneveld, H. J., Van Noortwijk, J. M., & Van Velzen, E. H. (1996). Analytical model for hydraulic roughness of submerged vegetation. In *Proceedings Of The Congress-International Association For Hydraulic Research* (pp. 775-780). Local Organizing Committee Of The XXV Congress.

Kubrak, E., Kubrak, J., & Rowinski, P. M. (2008). Vertical velocity distributions through and above submerged, flexible vegetation. *Hydrological sciences journal*, *53*(4), 905-920.

Lamiot (2017). *Stuckenia pectinata* "Les Baillons" (river) à Enquin-sur-Baillons (Canche basin in département Pas-de-Calais (France). Retrieved from https://commons.wikimedia.org/wiki/File:Potamot_pectiné_Stuckenia_pectinata_dans_"Les_Baillons"_à_Enquin-sur-Baillons_03.jpg on 20.09.2018

Li, S. S., & Millar, R. G. (2011). A two-dimensional morphodynamic model of gravel-bed river with floodplain vegetation. *Earth Surface Processes and Landforms*, 36(2), 190-202.

Liu, D., Diplas, P., Fairbanks, J. D., & Hodges, C. C. (2008). An experimental study of flow through rigid vegetation. *Journal of Geophysical Research: Earth Surface*, *113*(F4).

Lopez, F., Garcia, M. (1997). *Open Channel Flow through Simulated Vegetation: Turbulence Modelling and Sediment Transport.* Hydrosystems Laboratory, Department of Civil Engineering, University of Illinois.

Madsen, J. D., Chambers, P. A., James, W. F., Koch, E. W., & Westlake, D. F. (2001). The interaction between water movement, sediment dynamics and submersed macrophytes. *Hydrobiologia*, 444(1-3), 71-84.

Maine, M. A., Sune, N., Hadad, H., Sánchez, G., & Bonetto, C. (2006). Nutrient and metal removal in a constructed wetland for wastewater treatment from a metallurgic industry. *Ecological Engineering*, *26*(4), 341-347.

Marcogliese, D. J., Blaise, C., Cyr, D., De Lafontaine, Y., Fournier, M., Gagné, F., ... & Hudon, C. (2015). Effects of a major municipal effluent on the St. Lawrence River: A case study. *Ambio*, 44(4), 257-274.

Marjoribanks, T. I., Hardy, R. J., & Lane, S. N. (2014a). The hydraulic description of vegetated river channels: the weaknesses of existing formulations and emerging alternatives. *Wiley Interdisciplinary Reviews: Water*, *1*(6), 549-560.

Marjoribanks, T. I., Hardy, R. J., Lane, S. N., & Parsons, D. R. (2014b). High-resolution numerical modelling of flow-vegetation interactions. *Journal of Hydraulic Research*, *52*(6), 775-793.

Marjoribanks, T. I., Hardy, R. J., Lane, S. N., & Tancock, M. J. (2017). Patch-scale representation of vegetation within hydraulic models. *Earth Surface Processes and Landforms*.

Martin, S., O. Champoux et J. Morin. (2016). *Modélisation des masses d'eau du fleuve Saint-Laurent au lac Saint-Pierre en support au suivi de la qualité de l'eau*. Note technique NT-118, Service météorologique du Canada, Environnement et Changement climatique Canada, Québec. 30 pages.

Matte, P., Secretan, Y., & Morin, J. (2017). Hydrodynamic modeling of the St. Lawrence fluvial estuary. I: Model setup, calibration, and validation. *Journal of Waterway, Port, Coastal, and Ocean Engineering*, *143*(5), 04017010.

Morin, J., Boudreau, P., Secretan, Y., & Leclerc, M. (2000a). Pristine lake Saint-François, St. Lawrence River: hydrodynamic simulation and cumulative impact. *Journal of Great Lakes Research*, *26*(4), 384-401.

Morin, J., Champoux, O., Mingelbier, M., Bechara, J. A., Secretan, Y., Jean, M., & Frenette, J. J. (2003). Emergence of new explanatory variables for 2D habitat modelling in large rivers: the St. Lawrence experience. *Canadian Water Resources Journal*, *28*(2), 249-272.

Morin, J., Leclerc, M., Secretan, Y., & Boudreau, P. (2000b). Integrated two-dimensional macrophytes-hydrodynamic modeling. *Journal of Hydraulic Research*, *38*(3), 163-172.

Munson, B. R., Young, D. F., Okiishi, T. H., & Huebsch, W. W. (2009). *Fundamentals of fluid mechanics*. 6th ed., John Wiley & Sons.

Murphy, E., Ghisalberti, M., & Nepf, H. (2007). Model and laboratory study of dispersion in flows with submerged vegetation. *Water Resources Research*, *43*(5).

Nikora, V., Larned, S., Nikora, N., Debnath, K., Cooper, G., & Reid, M. (2008). Hydraulic resistance due to aquatic vegetation in small streams: field study. *Journal of hydraulic engineering*, *134*(9), 1326-1332.

Nepf, H. M. (2012a). Flow and transport in regions with aquatic vegetation. *Annual Review of Fluid Mechanics*, *44*, 123-142.

Nepf, H. M. (2012b). Hydrodynamics of vegetated channels. *Journal of Hydraulic Research*, *50*(3), 262-279.

Nezu, I., & Sanjou, M. (2008). Turburence structure and coherent motion in vegetated canopy open-channel flows. *Journal of hydro-environment research*, *2*(2), 62-90.

Nikora, V., Larned, S., Nikora, N., Debnath, K., Cooper, G., & Reid, M. (2008). Hydraulic resistance due to aquatic vegetation in small streams: field study. *Journal of hydraulic engineering*, *134*(9), 1326-1332.

O'Hare, M. T., Hutchinson, K. A., & Clarke, R. T. (2007). The drag and reconfiguration experienced by five macrophytes from a lowland river. *Aquatic Botany*, *86*(3), 253-259.

Okamoto, T., & Nezu, I. (2010). Resistance and turbulence structure in open-channel flows with flexible vegetations. *Environmental Hydraulics, Two Volume Set*, 215-220.

Pasche, E. (1984). Turbulence Mechanism in Natural Streams and the Possibility of its Mathematical Representation. (in German) *Mitteilungen Instiut für Wasserbau und Wasserwirtschaft* No. 52. RWTH Aachen.

Petryk, S., & Bosmajian III, G. (1975). Analysis of flow through vegetation. *Journal of the Hydraulics Division*, *101*(ASCE# 114517 Proceeding).

Pitlo R.H., Dawson F.H. (1990). Flow resistance of aquatic weeds. In Aquatic Weeds: The Ecology and Management of Nuisance Aquatic Vegetation, Pieterse AH, Murphy KJ (eds). *Oxford University Press: Oxford*; 74–84.

Ramsar Sites Information Service. (n.d.). Retrieved March 27, 2017, from https://rsis.ramsar.org/ris/949

Raupach, M. (1992). Drag and drag partition on rough surfaces. *Boundary-Layer Meteorology*, *60*(4), 375-395.

Ree, W. O., & Crow, F. R. (1977). Friction factors for vegetated waterways of small slope. *Report ARS-S-151 January 1977. 61 p, 57 fig, 34 tab.*

Rennie, M. D., & Jackson, L. J. (2005). The influence of habitat complexity on littoral invertebrate distributions: patterns differ in shallow prairie lakes with and without fish. *Canadian Journal of Fisheries and Aquatic Sciences*, 62(9), 2088-2099.

Righetti, M. (2008). Flow analysis in a channel with flexible vegetation using double-averaging method. *Acta Geophysica*, 56(3), 801.

Roy, L. (2002). Les impacts environnementaux de l'agriculture sur le Saint-Laurent. *Le Naturaliste canadien*, *126*(1), 67-77.

Sand-Jensen, K. (2003). Drag and reconfiguration of freshwater macrophytes. *Freshwater Biology*, *48*(2), 271-283.

Schlichting, H. (1936). Experimental investigation of the problem of surface roughness. NASA Technical Memorandum 823, Washington, DC.

Schmieder, K., Werner, S., & Bauer, H. G. (2006). Submersed macrophytes as a food source for wintering waterbirds at Lake Constance. *Aquatic Botany*, 84(3), 245-250.

Secretan, Y., & Dubos, V. (2005). Modélisation de la variabilité verticale des vitesses dans un modèle hydrodynamique 2D horizontal. *Revue Européenne des Eléments*, *14*(1), 115-138.

Sharpe, R. G., & James, C. S. (2006). Deposition of sediment from suspension in emergent vegetation. *Water SA*, 32(2), 211-218.

Statzner, B., Lamouroux, N., Nikora, V., & Sagnes, P. (2006). The debate about drag and reconfiguration of freshwater macrophytes: comparing results obtained by three recently discussed approaches. *Freshwater Biology*, 51(11), 2173-2183.

Stone, B. M., & Shen, H. T. (2002). Hydraulic resistance of flow in channels with cylindrical roughness. *Journal of hydraulic engineering*, *128*(5), 500-506.

Talbot, A. (2006). Enjeux de la disponibilité de l'eau pour le fleuve Saint-Laurent Ŕ Synthèse environnementale. *Environnement Canada, Montréal*.

Tall, L., Caraco, N., & Maranger, R. (2011). Denitrification hot spots: dominant role of invasive macrophyte Trapa natans in removing nitrogen from a tidal river. *Ecological Applications*, 21(8), 3104-3114.

Tanino, Y., & Nepf, H. M. (2008). Laboratory investigation of mean drag in a random array of rigid, emergent cylinders. *Journal of Hydraulic Engineering*, *134*(1), 34-41.

Thomaz, S. M., Dibble, E. D., Evangelista, L. R., Higuti, J., & Bini, L. M. (2008). Influence of aquatic macrophyte habitat complexity on invertebrate abundance and richness in tropical lagoons. *Freshwater biology*, 53(2), 358-367.

Tsujimoto, T., Shimizu, T., Okada, T. (1991). Turbulent Structure of Flow over Rigid Vegetation-Covered Bed in Open Channels. *KHL Progressive Report 1.* Hydraulic Laboratory, Kanazawa University, Japan.

Vargas-Luna, A., Crosato, A., & Uijttewaal, W. S. (2015). Effects of vegetation on flow and sediment transport: comparative analyses and validation of predicting models. *Earth Surface Processes and Landforms*, *40*(2), 157-176.

Velasco, D., Bateman, A., & Medina, V. (2008). A new integrated, hydro-mechanical model applied to flexible vegetation in riverbeds. *Journal of Hydraulic Research*, *46*(5), 579-597.

Verschoren, V., Meire, D., Schoelynck, J., Buis, K., Bal, K. D., Troch, P., ... & Temmerman, S. (2016). Resistance and reconfiguration of natural flexible submerged vegetation in hydrodynamic river modelling. *Environmental Fluid Mechanics*, 16(1), 245-265.

Vila-Costa, M., Pulido, C., Chappuis, E., Calviño, A., Casamayor, E. O., & Gacia, E. (2016). Macrophyte landscape modulates lake ecosystem-level nitrogen losses through tightly coupled plant-microbe interactions. *Limnology and Oceanography*, 61(1), 78-88.

Vis, C., Cattaneo, A., & Hudon, C. (2008). Shift from chlorophytes to cyanobacteria in benthic macroalgae along a gradient of nitrate depletion 1. *Journal of Phycology*, 44(1), 38-44.

Wilson, C. A. M. E., & Horritt, M. S. (2002). Measuring the flow resistance of submerged grass. *Hydrological Processes*, *16*(13), 2589-2598.

Wilson, C. A. M. E. (2007). Flow resistance models for flexible submerged vegetation. *Journal of Hydrology*, *342*(3), 213-222.

White, B. L., Ghisalberti, M., & Nepf, H. M. (2004). Shear layers in partially vegetated channels: Analogy to shallow water shear layers. Shallow Flows, 267-273.

Wu, F. C., Shen, H. W., & Chou, Y. J. (1999). Variation of roughness coefficients for unsubmerged and submerged vegetation. *Journal of Hydraulic Engineering*, *125*(9), 934-942.

Wunder, S., Lehmann, B., & Nestmann, F. (2011). Determination of the drag coefficients of emergent and just submerged willows. *International journal of river basin management*, *9*(3-4), 231-236.

Yan, J. (2008). Experimental study of flow resistance and turbulence characteristics of open channel flow with vegetation. *China: Hohai University*.

Yang, W. (2008). *Experimental study of turbulent open-channel flows with submerged vegetation* (Doctoral dissertation, Ph. D. thesis, Yonsei University, Korea).

Yang, W., & Choi, S. U. (2010). A two-layer approach for depth-limited open-channel flows with submerged vegetation. *Journal of Hydraulic Research*, *48*(4), 466-475.